CHALMERS

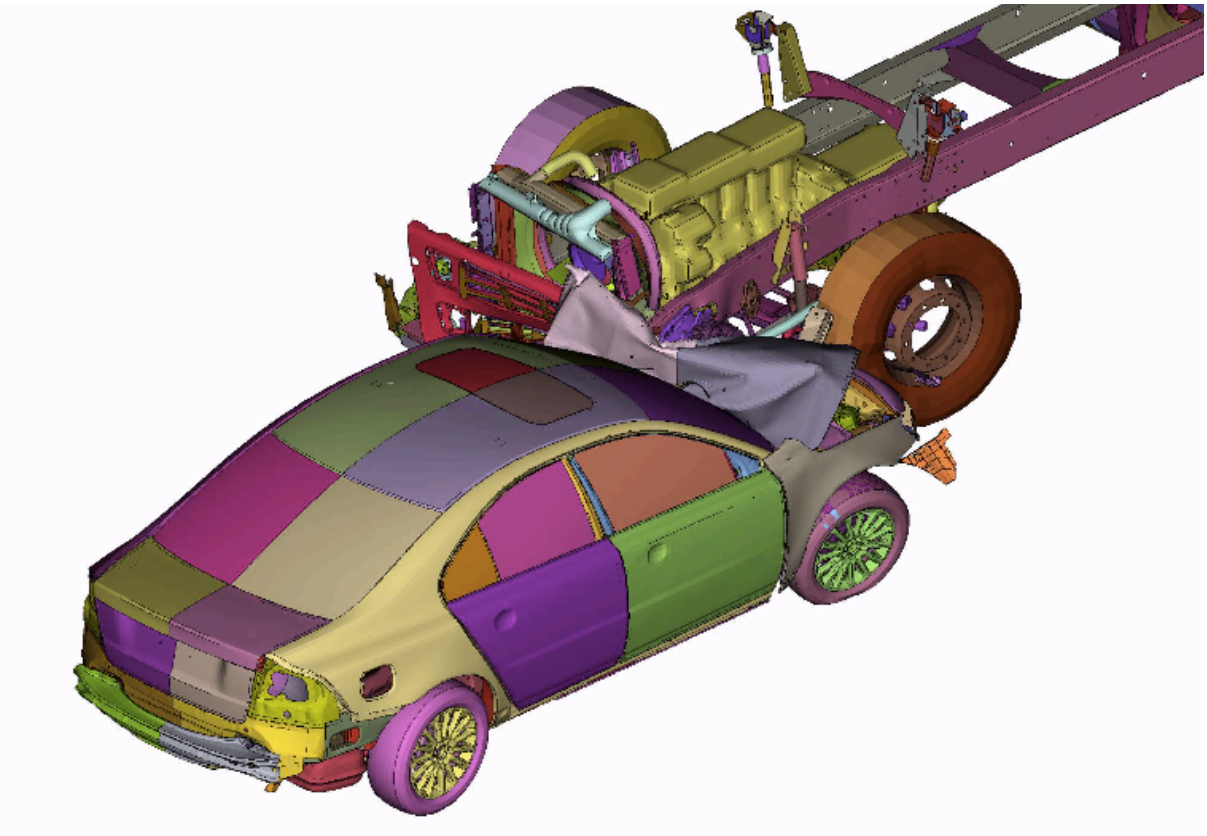

Car-to-Truck Frontal Crash Compatibility

Quantification of the possible crash severity reduction from an additional truck frontal structure

Master's Thesis in the Automotive Engineering Master

BERTRAND LEFER - IVAN REBOLLOSO

Department of Applied Mechanics
Division of Vehicle Safety
CHALMERS UNIVERSITY OF TECHNOLOGY
Göteborg, Sweden 2012
Master's thesis 2012:25

MASTER'S THESIS IN AUTOMOTIVE ENGINEERING

Car-to-Truck Frontal Crash Compatibility

Quantification of the possible crash severity reduction from an additional truck frontal structure

BERTRAND LEFER – IVAN REBOLLOSO

Department of Applied Mechanics
Division of Vehicle Safety
CHALMERS UNIVERSITY OF TECHNOLOGY
Göteborg, Sweden 2012

Car-to-Truck Frontal Crash Compatibility
Quantification of the possible crash severity reduction from an additional truck frontal structure

BERTRAND LEFER – IVAN REBOLLOSO

Master's Thesis 2012:25
ISSN 1652-8557
Department of Applied Mechanics
Division of Vehicle Safety
Chalmers University of Technology
SE-412 96 Göteborg
Sweden
Telephone: + 46 (0)31-772 1000

Cover:
Simulation of a Volvo S80 crashing into a heavy truck. Impact speed: 65km/h. Horizontal overlap: 50% of the truck.

Chalmers Reproservice
Göteborg, Sweden 2012

Car-to-Truck Frontal Crash Compatibility

Quantification of the possible crash severity reduction from an additional truck frontal structure

Master's Thesis in the Automotive Engineering Master

BERTRAND LEFER – IVAN REBOLLOSO
Department of Applied Mechanics
Division of Vehicle Safety
Chalmers University of Technology

ABSTRACT

For the last five years, are average of 38 500 people have been killed each year in Europe in road traffic accidents and, even if Heavy Goods Vehicles represent only 1% of the vehicle registered, they have been involved in more than 5000 fatal accidents in 2009. Among these accidents involving trucks, 65% involved the truck front.

The severity of these crashes can be explained by the large mass difference between cars and trucks that inevitably leads to higher deceleration pulses for the passenger car; most of times followed by major deformations of the car passenger compartment. In the worse frontal crash cases, the car ends under the truck.

To reduce the risk of trucks overriding passenger cars and reduce the crash severity, so-called Front Underrun Protection Systems have been developed and are now compulsory on new trucks in Europe. The efficiency of these systems has been proved by different studies but it has also been shown that they could be even more efficient if their energy absorption could be increased for instance by increasing the deformation length.

The purpose of this thesis work was therefore to quantify the possible crash severity reduction, mainly for the car occupants, from an additional truck frontal structure in case of frontal crash between cars and trucks and to make recommendations on a new front structure of heavy trucks that can have an injury reducing potential for car occupants. In this study the length, the stiffness and the basic design of this new truck front structure have been investigated. The study has been made mainly using Finite Element simulations but also using analytical calculations.

The results confirm that the use of a longer energy absorbing structure in front of the truck would decrease the crash severity for the car occupants while experiencing a frontal crash with a truck. The critical impact speeds are increased since the new truck structure is absorbing much more energy than current Front Underrun Protection Systems. Because of the new frontal structure load distribution, the forces that need to be carried by the truck front structure are also lowered.

Key words: Traffic safety, frontal impacts, crash compatibility, crash pulses, frontal structures for trucks, heavy vehicles, underrun, FUPS, Finite Element.

Contents

Preface

This report is the result of the master thesis work carried out in the Cab Analysis Group at Volvo Group Trucks Technology (Volvo GTT), Göteborg. This thesis fulfils the partial requirement for the Master of Science degree in "Automotive Engineering" at Chalmers University of Technology, Göteborg, Sweden. This thesis work was started in June 2011 and finished in May 2012.

The main motivation behind performing this thesis work has been to develop a novel frontal structure for a HGV in order to reduce the crash severity for the passengers of cars experiencing a frontal crash with a truck. The outcomes of this work provide an initial guideline for the future development of an effective truck crash nose that could leads to a fatality reduction on the roads.

We would like to thank Mr Matti Koponen, Group Manager, for giving the opportunity and all the necessary resources for carrying out this thesis work in his group. We would also like to thank Mr Peter Rundberget and Mr Fredrik Törnvall for being our supervisors during the entire period of this thesis work. Their timely and good guidance have helped to make this thesis as much interesting as possible for us but also for Volvo GTT through our results. We would also like to thank Mr Linus Wågström, from Volvo Car Corporation (VCC), Göteborg, for helping us out with various aspects during this past year spent on the thesis. We would like to show our gratitude to Mr Göran Peterson and Björn Cognell who have helped sharing their experiences about Finite Element simulations. Finally, we thank Professor Karin Brolin for being our examiner at Chalmers University and having spent time for advising us.

Göteborg, May 2012

Bertrand Lefer & Ivan Rebolloso

Notations

Abbreviations

CFC	Channel Frequency Class
FCC	Frontal Crash Criterion
FE	Finite Element
FF35 (35mph)	Full Frontal crash test in a rigid wall with a closing speed of 56km/h
FHT	Flexible Heavy Truck
FMVSS	Federal Motor Vehicle Safety Standards
FUPS	Front Underrun Protection System
IIHS	Insurance Institute for Highway Safety
HC	Honeycomb
HGV	Heavy Goods Vehicles
MDB	Moving Deformable Barrier
NCAP	New Car Assessment Programme
OLC	Occupant Load Criterion
RHT	Rigid Heavy Truck
VCC	Volvo Car Corporation

Symbols with corresponding units

a(t)	Acceleration as a function of time [m/s^2]
d_{max}	Maximum deformation [m]
d(t)	Mass displacement as a function of time (in the OLC model) [m]
D(t)	Car displacement as a function of time [m]
$E_{d,i}$	Deformation energy of the entity "i" [kJ]
$E_{k,i}$	Kinetic energy of the entity "i" [kJ]
$E_{k,r}$	Residual kinetic energy [kJ]
F_{max}	Maximum deformation force [N]
F_0	Constant restrain force [N]
F(X)	Force as a function of X [N]
m_i	Mass of the entity "i" [kg]
t	Time [s]
v(t)	Velocity as a function of time [m/s]
V_0	Initial velocity [m/s]
X(t)	Mass-Car relative displacement as a function of time [m]

1 Motivation and Objectives

For the last five years, an average of 38 500 people have been killed each year in Europe in road traffic accidents and, even if Heavy Goods Vehicles (HGV) represent around 1% of the vehicle registered, they have been involved in more than 5000 fatal accidents in 2009 in EU-23[1] [1], which correspond to more than 12% of fatalities. In Sweden, heavy vehicles are involved in about 20% of fatal accidents whereas they represent less than 10% of the traffic [2]. Among these accidents involving trucks, 65% involved the truck front and nearly half of them involved the car front as well [3]. According to the Insurance Institute for Highway Safety (IIHS), 98% of US vehicle occupants killed in two-vehicles crashes that involved a large truck and a passenger car in 2009 were car occupants [4].

The large mass difference between cars and trucks inevitably leads to higher deceleration pulses for the passenger car; most of times followed by major deformations of the car passenger compartment.

To reduce the risk of trucks overriding passenger cars, so-called Front Underrun Protection Systems (FUPS) have been developed. These systems can provide the needed reaction force to enable energy absorption in passenger car frontal structures, nevertheless the amount of absorbed energy is limited. According to the European legislation (96/53/EC), the total length of the trucks is limited and therefore they are mostly designed to maximize the load space. This is why most European truck cabs are designed with a flat vertical surface in the front that results with a little space available between the front of the vehicle and the front axle, therefore the amount of energy that can be absorbed is limited [5].

In the UK, a consultation has been done about increasing the length of semi-trailers by 2,05m [6]. If such an increase would be allowed, the frontal crush zone of the trucks could be improved from the increase of the deformation length and therefore the amount of energy absorbed. The protection of vulnerable road users or the fuel consumption linked to the aerodynamics could also be improved.

The aims of the study presented in this report, were therefore to quantify the possible crash severity reduction, mainly for the car occupants, from an additional frontal structure in the truck and make recommendations on a new front structure of heavy trucks that can have an injury reducing potential for occupants of passenger cars. These recommendations concern the length, the stiffness, and the basic shape of this new truck front structure.

This study was mainly based on Finite Element (FE) simulations using the Volvo S80 car model and the Volvo FH truck model. Analytical calculations have also been made to estimate the improvements that could be expected from this new frontal structure.

The effects of the truck nose on vulnerable road users protection, aerodynamic improvement and manoeuvrability issues have not been included in the study.

---

[1] Belgium, Czech-Republic, Germany, Denmark, Ireland, Greece, Spain, France, Italy, Luxembourg, Netherlands, Austria, Poland, Portugal, Romania, Slovenia, Finland, Sweden, United Kingdom, Estonia, Latvia, Hungary, Slovakia

2 Background

2.1 Traffic safety

Since there are more and more road users in the world, the traffic safety has become a major subject of research for the past years. As it has been said, the number of people dying on the roads is a main concern and therefore a lot of efforts are made to offer the best protections to all the roads users by trying to develop vehicles that are safer. The crash compatibility between different size vehicles is also a major concern. For instance, crashes involving cars and HGV are often leading to severe injuries or death of the car occupants.

This study has been focussing on head-on collisions between cars and trucks. The large mass difference between those types of vehicle is one of the main reasons for the high severity of these crashes. Add to this, the front geometries are also very different and generate some incompatibility issues. For some years now, FUPS have been developed for the trucks in order to improve the car to truck crash compatibility and this thesis work aims to investigate how these FUPS could be improved in the future.

In this first subpart, a brief background description has been made for the reader to get a good understanding of the subject. This background starts with the crash theory basics explanation of the main principles used for the calculations. Then, a short description of the passenger car design from the safety point of view. The last part deals with the presentation of the truck FUPS.

The second subpart is a sum-up of the different studies that have already been made on the car to truck crash compatibility. First, about the truck FUPS effects on the crash severity and secondly about the efficiency improvement that could be resulting from an increased length of these truck underrun protection systems.

2.1.1 Crash theory

In a head-on collision involving two vehicles, the total initial kinetic energy ($E_{k,i}$) can be determined [5] & [7]. The mass and speed of the vehicle 1 and 2 are respectively called m_1, v_1 and m_2, v_2. Then the initial kinetic energy is given by

$$E_{k,i} = 0,5 \cdot (m_1 \cdot v_1^2 + m_2 \cdot v_2^2) \quad (2.1)$$

From the conservation of momentum principle and assuming that after crashing the two vehicles are moving together with the same residual speed v_3, the following equation can be written:

$$m_1 \cdot v_1 - m_2 \cdot v_2 = (m_1 + m_2) \cdot v_3 \rightarrow \; v_3 = \frac{m_1 \cdot v_1 - m_2 \cdot v_2}{(m_1 + m_2)} \quad (2.2)$$

This residual speed is due to the residual kinetic energy that is equal to

$$E_{k,r} = 0,5 \cdot (m_1 + m_2) \cdot v_3^2 \quad (2.3)$$

From these three equations, the dissipated energy used to deform both vehicles can be calculated. It is equal to the difference between the initial and residual energy.

$$E_d = E_{k,i} - E_{k,r} = \frac{1}{2} \cdot \frac{m_1 \cdot m_2}{m_1 + m_2} \cdot (v_1 + v_2)^2 \quad (2.4)$$

In this study, the truck was assumed to be stationary therefore the energy that needs to be absorbed is depending on the car speed before impact (v) and the mass of both vehicles: $E_d = \frac{1}{2} \cdot \frac{m_1 \cdot m_2}{m_1 + m_2} \cdot v^2$ (2.5)

This energy is dissipated by both the deformation of the car front and the truck front. The area under the force-displacement curve gives the absorbed energy of the car front structure. These curves can be extracted either from crash tests or also from the simulations. Typical force-displacement curves are shown Figure 2.1.

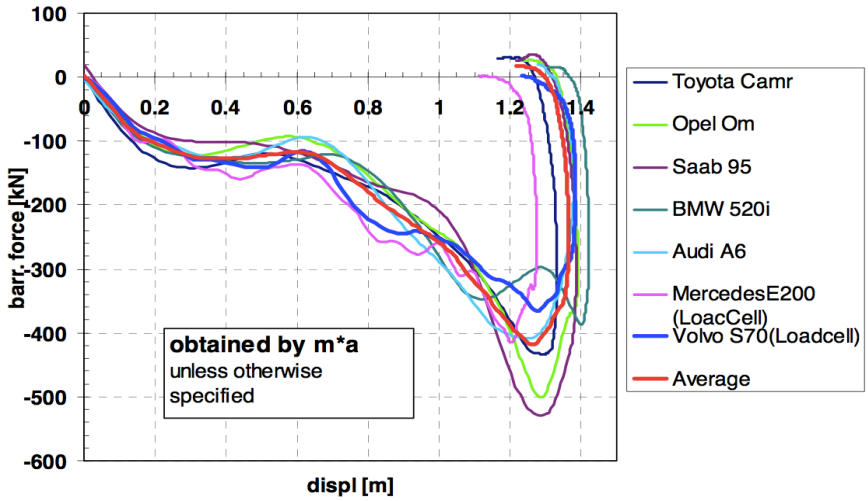

Figure 2.1 Example of force-displacement curves for a range of large saloon cars impacting a deformable barrier at 64 km/h (taken from Huibers and deBeer, [17])

Since these curves are quite complex, the car deformation can be approximated as a linear force/displacement relationship [5]. The force reaches a maximum value, F_{max}, while the displacement increases to a maximum deflection, d_{max}, the energy dissipated by the car deformation can be estimated to be

$$E_{d,car} = \frac{1}{2} \cdot F_{\max} \cdot d_{\max} \quad (2.6)$$

Assuming that the truck front structure is collapsing at a constant force level in respect to the deflection, the energy that would be absorbed by its deformation can be calculated from the equation (2.7).

$$E_{d,truck} = F_d \cdot d_{\max,2} \quad (2.7)$$

where F_d is the constant deformation force level of the truck front structure and $d_{max,2}$ the maximum deformation of this truck front structure.

2.1.2 Passenger car safety design

From the first car models, car design has evolved a lot. These evolutions were concerning aerodynamic, external design, production methods and safety. The safety part is probably one of the most important because it is directly linked to the occupant protection. This is why a lot of efforts are made to try to increase the car occupant protection while designing a new car model.

For years now, the car safety has become more and more important in the car development and the number of safety devices in cars hasn't stop increasing. Seatbelts, airbags, or other active safety systems have been integrated in cars to protect their occupants for different crash configurations as frontal impact, side impact, rear impact or from rollover. To achieve this goal, the car body structure is also designed to be as safe as possible with some crushing zones to absorb energy but also a stiff protective cell for the occupants so called safety cage, see Figure 2.2.

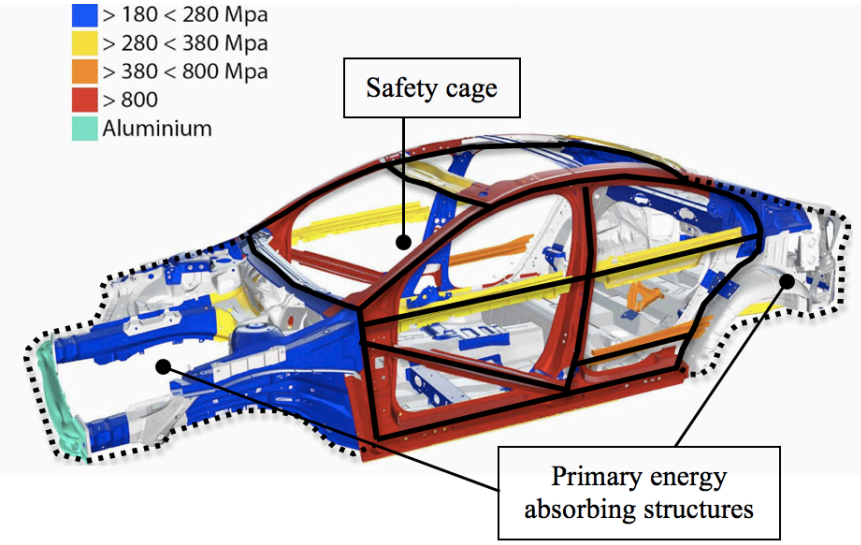

Figure 2.2 Example of a state-of-the art vehicle structure [8]

The main energy-absorbing zones are situated in the front and rear parts of the cars, see Figure 2.2; they are designed in order to have a controlled deformation. This deformation is used to absorb the maximum kinetic energy during a crash. The absorbed energy can be quantified using the equation (2.6). The deformation zones are designed to absorb the kinetic energy of the car itself, for instance from a full frontal crash into a rigid wall [9].

In this configuration, the ideal would be that the car doesn't rebound after crashing in the wall meaning that the whole energy has been absorbed and therefore the velocity change is the lowest possible. But these energy absorbing zones should also be able to deform while crashing with a lighter car for example, then the triggering force needed to start deforming the structures has to be lower than the maximum peak force than the smaller car can produce. This is why these structures are divided in different zones having different crush strengths.

On the contrary to the energy absorbing structures, the safety cage is built with high-strength material that should not be deformed. This zone is the principal part of the safety structure that is completed with the energy absorbing zones. In case of crash, it is designed to create a survival cell around the occupants preventing intrusion.

Different consumer rating test programmes quantify this occupant protection level; the most common are the EURO-NCAP and US-NCAP.

2.1.3 Truck Front Underrun Protection Systems

While a car is crashing with a truck, the severity of the crash for the passenger car occupants is often high because of different incompatibility problems. The first is the

large weight difference between these two types of vehicle, therefore the kinetic energy of the truck is much higher than the one of the car [10]. This high kinetic energy leads to higher velocity change for the car and therefore a higher crash pulse. The second incompatibility is geometrical due to the different sizes and dimensions. For instance the bumper heights are different and because of this, if nothing is done, the passenger car can slide under the truck front in case of crash. Add to this, if the front deformable zone of the car doesn't hit the truck bumper properly, the energy absorption due to the car frontal deformation will decrease.

To solve these incompatibility problems, different underrun protection systems have been developed for the different truck zones, front, rear or side. Since August 2003, a European directive (2000/40/EC, ECE R93) rules the geometry and static legal demand of these FUPS, see Figure 2.4. Since this date, these systems are compulsory on new heavy vehicles.

About FUPS, their aim is to prevent the car to crush under the truck or bus and also to engage the deformation of the car front structure [10]. An example of FUPS can be seen Figure 2.3.

Nowadays, mainly two different types of FUPS are used. The first type is a rigid or quasi-rigid barrier that is just preventing the car to underrun the truck but also engaging the energy absorbing parts of the car. The second type is a so-called energy-absorbing FUPS (ea-FUPS). The main difference is that this kind of device is deformable and therefore can be part of the energy dissipation during the crash. They are built in a way that the structure can be deformed but still catch the car.

Figure 2.3 Example of FUPS mounted on a Volvo bus [11]

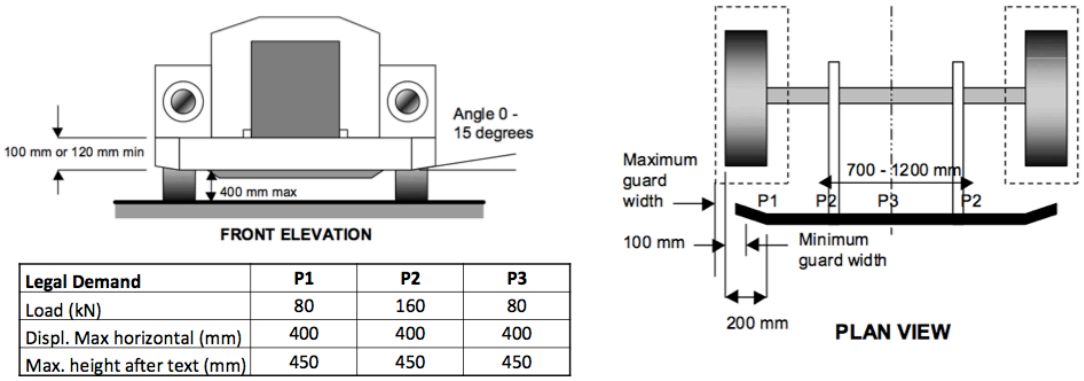

Legal Demand	P1	P2	P3
Load (kN)	80	160	80
Displ. Max horizontal (mm)	400	400	400
Max. height after text (mm)	450	450	450

Figure 2.4 Strength requirements for FUPS according to 2000/40/EC [12]

"In Europe, an estimate is 800 saved lives per year if all trucks were equipped" (by an effective FUPS) [13].

2.2 Previous studies

2.2.1 Front Underrun Protection Systems

Different studies have been investigating the effect of FUPS on the crash severity.

From 2003 to 2006, the project VC-Compat (Vehicle Crash Compatibility) was carried by different partner organisations (automotive and truck manufacturers, transport organisations and universities) [14]. A part of this study was investigating with the relationship between injuries of the passenger car occupants and the efficiency of truck FUPS. The aim was to show that these structures prevent underride, improve car to truck compatibility and can decrease the passenger injuries with an added energy absorption.

From crash tests between different car models and FUPS systems (rigid or energy absorbing), their conclusions were that in all cases underride was prevented and the energy absorption has decreased the maximum deceleration of the passenger car. The absorbed energy is limited due to the low deformation distance available for the FUPS therefore an increased available length could improve its efficiency.

In the study, it has been estimated that the force generated by the car in an offset configuration crash is between 200 and 300kN. It was also estimated that experiencing a 72% overlap head-on crash up to 75 km/h with a small family car, the passenger would not be submitted to severe injuries if the truck is equipped of an ea-FUPS.

In 2010, a study by Krusper and Thomson [15] was carried about ea-FUPS. Using FE simulations, they have investigated the theoretical performance of ea-FUPS interacting with the front end of passenger cars in different impact configurations (rigid wall or simplified ea-FUPS model). Their results show that for an impact speed of 75 km/h, the car sill and firewall deformations are less when impacting the ea-FUPS comparing to a rigid wall. The energy absorbed by the ea-FUPS was shown to be up to 34% of the total kinetic energy even if the interaction surface with the car front is smaller. Because of this energy absorption, the crash pulse can be decreased and thereby lowering the injury risk assuming no intrusion in the safety cage. They also concluded that one of the important parameter influencing the car to truck interaction is the crushing force level needed to activate the truck front structure deformation. Therefore the determination of this force level is very important while developing a FUPS.

In 2003, Forsman [13] presented the design of the new FUPS for the Volvo FH and FM. This truck front structure has been designed to comply with the European legal demands, ECE R93, for FUPS. Moreover, to reduce the pulse for a passenger car with a closing speed of 65 km/h and a 75% car overlap. Add to this, the structure is rigid enough to withstand the force from a larger car in the same configuration. The optimisation of the FUPS has been done by changing the crumpling tubes connecting the FUPS to the rigid parts of the truck chassis. It was conclude that the efficiency of this structure is limited by the available space and also that the weight increase should be minimized not to overload the front axle.

2.2.2 Estimated effects of an increased deformation length

In many studies about FUPS, one main conclusion is that the efficiency of truck underrun protection systems is limited by the deformation length and that if they could be longer, the absorbed energy would be higher and therefore the passenger car occupant protection improved. One part of the research that has been conducted by the Transport Research Laboratory in 2010 was about estimating the effects of an increased deformation length of FUPS [5]. One of their objectives was to quantify, using analytical methods, the potential benefits of different lengths of truck front structure for the safety of car occupants.

They have been calculating the energy that could be absorbed by these different new front structures up to an increased length of 2250 mm and then also calculated what would be the critical impact speed for each different case. This critical impact speed is defined as the maximum closing speed for which both the car and truck crumple zones can absorb all the impact energy. For all the tests, the truck crumple zone had a constant crushing force of 250kN.

In order to estimate the energy that would be absorbed by the truck front structure, it has been considered as collapsing at a constant force level in respect to its deformation. The energy dissipated by the truck nose deformation can be calculated from the equation (2.7).

The study was focused on three different car models, small, medium and large, and three different truck models (12 tonnes, 25 tonnes and 44 tonnes), that has given nine different crash configurations. For each of them the critical impact velocity has been calculated, the results can be seen in Figure 2.5.

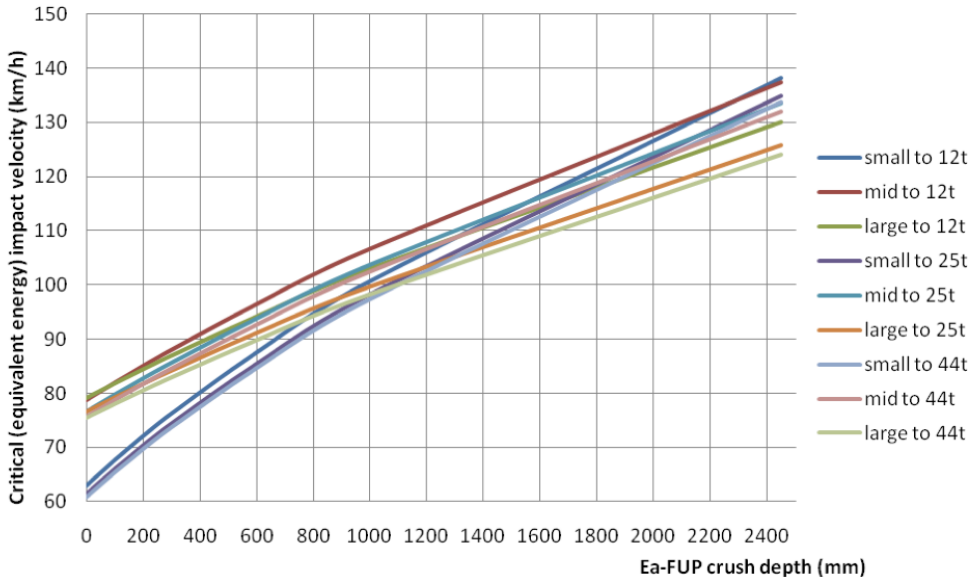

Figure 2.5 Critical (equivalent energy) impact speeds at various ea-FUPS crush depths (taken from TRL PPR533 [5])

The Transport Research Laboratory study [5] has shown that without increasing the length of the truck but by using a 200 mm-length ea-FUPS under the existing cab, the critical speed could be increased from about 60 to 70 km/h for the small car and from about 79 to 85 km/h for the large one.

By increasing the length of the truck by 800 mm, corresponding to an ea-FUPS length of 1m, critical speeds could be increased to about 95-105 km/h and if the truck length were increased by 2250 mm, the critical speeds would be around 125-135 km/h.

Scania has presented a project in 2003 with an increased front nose of 600 mm (and 250kg) that was said to be able to increase the critical impact speed from 56 to 80 km/h in a frontal car to truck crash. Scania has estimated that this speed increase could save 900 lives a year [16].

3 Methodology

For this study, two different approaches have been used. The first one was to use an analytical method based on the crash theory, all the calculations have been done using Microsoft Excel. The second and main approach was to use FE models and simulations. For this part of the study different software have been used. The models have been created using ANSA 64Bit (version 13.1.5) and HyperCrash (version 10), the simulations have been run with RADIOSS (version 1004). The post-processing software used to analyse the simulation results was MetaPost (version 6.6.4).

3.1 Analytical method

As it has been done in the study published by the Transport Research Laboratory (TRL) in 2010 [5] (see Section 2.2.2), it was decided to estimate the potential benefits of an increased truck front structure using the same analytical method used in the TRL study [5] but with the Volvo S80 model. In order to do so, the maximum energy absorbed by the car used in that study had to be estimated. This has been done from the simulation of the Volvo S80 model crashing in a rigid wall, with 75% overlap and a closing speed of 75 km/h. This speed has been chosen since it was the one at which the car front deformation zones were fully deformed. That is to say that the maximum energy absorption of the car has been reached (in this simulation, the rigid wall has the same size and position that the additional honeycomb structure used later). The estimation of the maximum absorbed energy by the car has been estimated using two different methods.

The first one was to extract the energy absorbed by the car from the post-processing tool "MetaPost". The second method was to use the model of a linear force-displacement characteristic of the car front structure [17]. From the simulation results, the force-displacement curve can be plotted. From this curve, the maximum displacement and crush force were determined and therefore the energy absorbed calculated from equation (2.6).

With this estimation of the car maximum energy absorption, the maximum energy that can be absorbed has been calculated since it is the sum of the one absorbed by the car deformation (determined above) and the one absorbed by the truck nose calculated from equation (2.7).

Now that the maximum energy that can be absorbed during the crash is known, from both the car and the truck deformations, the critical impact speed can be calculated using the equation bellow (deducted from equation (2.5)):

$$v = \sqrt{2 \cdot E_d \cdot (\frac{m_{car} + m_{truck}}{m_{car} \cdot m_{truck}})} = \sqrt{2 \cdot (E_{d,car} + F_d \cdot d_{\max}) \cdot (\frac{m_{car} + m_{truck}}{m_{car} \cdot m_{truck}})} \quad (3.1)$$

This speed has been calculated for the Volvo S80 model and for a truck energy absorbing structure length (d_{max}) from 0 to 2500 mm. Different truck nose crush forces have been used also from 250 to 500kN. Since the new frontal truck nose should be compatible with different weight range of cars, at least a part of it needs to have a crushing force compatible with the force peak that can be reached during lighter car crashes. These results have been used to get a rough estimate of what could be expected from the simulation results.

Once the different models of the honeycomb structure have been optimised, the energy absorbed from their deformation was known. Therefore, the total maximum

deformation energy has been estimated as well as the critical speeds using equation (3.1) and compared with the theoretical critical speeds from the constant crushing force model explained just before.

3.2 Finite Element models

3.2.1 FE models provided

- **Truck (flexible and rigid)**

Two different truck FE models have been used, both provided by Volvo Group Trucks Technology (Volvo GTT). The two models were representing a simplified model of the current Volvo FH truck model. The truck cabin geometry was not modelled, see Figure 3.1.

The model consisted of 325046 nodes and 301917 elements (60% shell element and 38% brick elements). The total weight of the model was 12000kg. The difference between the two truck models was that the second was modelled as a rigid body that cannot be deformed whereas the first model was flexible. For both models, the truck rear beams could be fixed that had for effect to provide the truck to move backward during the crash representing an infinitely loaded truck.

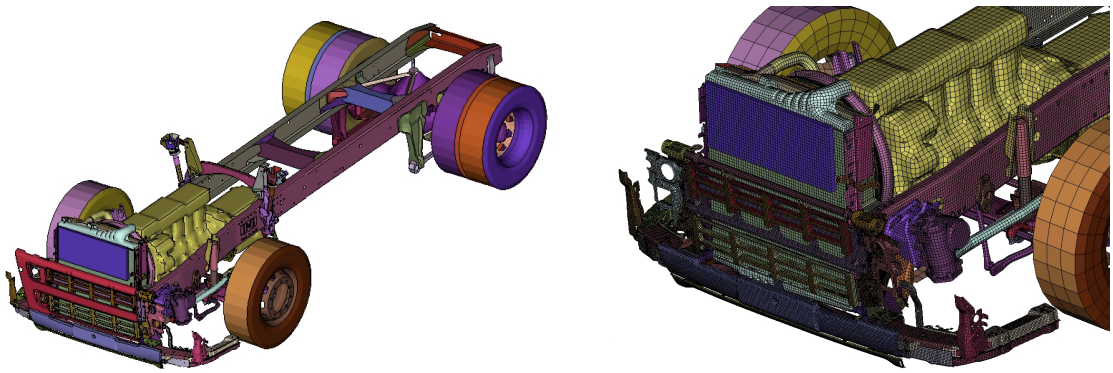

Figure 3.1 Volvo FH truck finite element model

- **Volvo S80**

A complete Volvo S80 FE model (provided by VCC) has been used to develop the optimal crash nose, all the main components are included with the exception of the front plastic bumper which was removed to facilitate the analysis, see Figure 3.2. Also, the airbags and seatbelts are not modelled.

The model was made up of 658282 nodes and 652226 elements (96% shell elements) with a total mass of 1991kg.

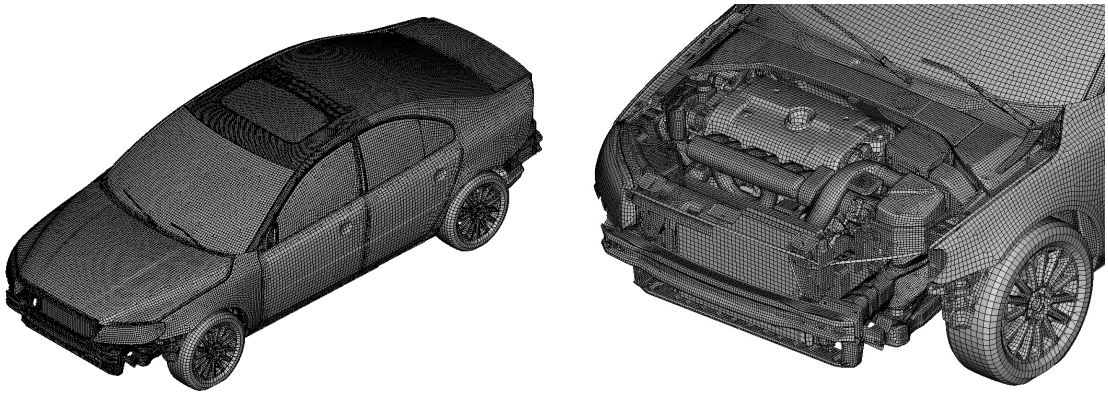

Figure 3.2 Volvo S80 finite element model

3.2.2 FE models created

- **Additional truck frontal structure models**

The energy absorption structure was based on the Federal Motor Vehicle Safety Standards (FMVSS) No. 214 Moving Deformable Barrier (MDB). In order to have a robust model it was decided to divide it in two sections, the first section (60 mm thick) corresponds to the "bumper element honeycomb material" to ensure the load distribution at the front plate by having a stiffer material. The second part of the structure is the "main honeycomb block material" [18] for a total length of 900 mm, see Figure 3.3. According to the material specification, the crush strength for the main honeycomb material is set to 0,310MPa and 1,690MPa for the bumper honeycomb material. More details about the honeycomb materials are shown in Appendix 8.1.

Two steel plates (front and back) are used as support for the honeycomb material and for the load distribution (no adhesive elements in between were considered).

The model was made up of 146880 nodes and 143820 elements: 95,7% brick elements (35kg for the honeycomb) and 4,3% shell elements (57kg for the steel plates). The total mass of the additional structure was 92kg.

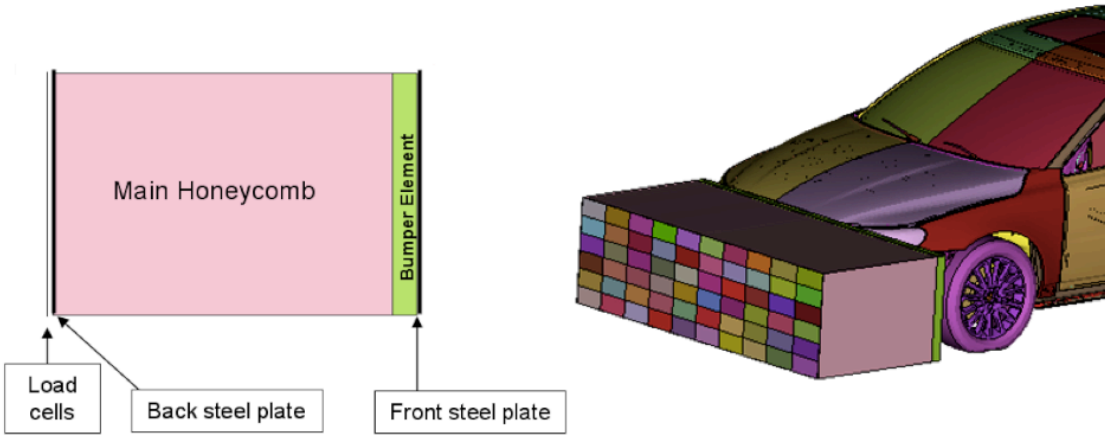

Figure 3.3 Honeycomb crash nose model

In order to capture the load distribution on the back plate, an additional load cell plate has been added at the rear of the structure. This plate is composed of 60 load cells, see Figure 3.4 and made up with 3060 shell elements for a weight of 29kg.

Each load cell is used to capture the forces during the collision from which the maximum values in tension and compression have been measured. With these values it was possible to identify the critical points in term of force peak for each load case.

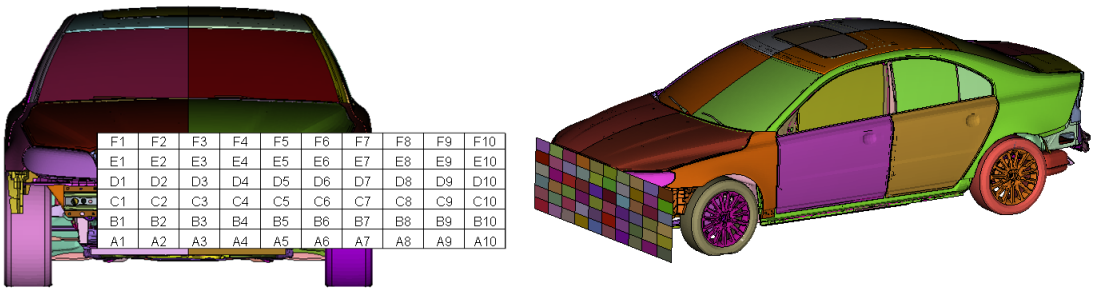

Figure 3.4 Load cell distribution for a 75% overlap without honeycomb structure

Four other crash nose models have been created from the one described above. For the two first, only the honeycomb length has been changed to 600 mm and 300 mm.

The 600 mm-length crash nose model was made up of 98983 nodes and 97920 elements: 93,7% brick elements (25kg for the honeycomb) and 6,3% shell elements (57kg for the steel plates). The total mass of this model was 82kg.

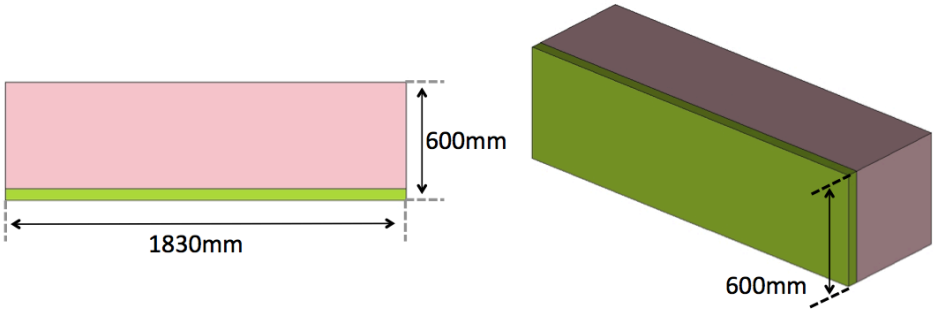

Figure 3.5 600 mm-length honeycomb crash nose model (top and iso views)

The 300 mm-length crash nose model was made up of 51088 nodes and 52020 elements: 88% brick elements (14,5kg for the honeycomb) and 12% shell elements (57kg for the steel plates). The total mass of this model was 71,5kg.

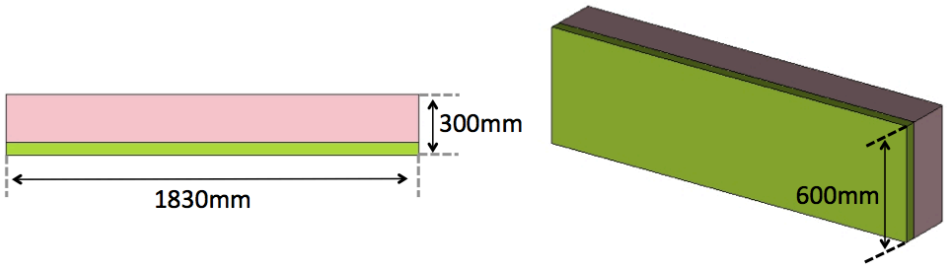

Figure 3.6 300 mm-length honeycomb crash nose model (top and iso views)

For the third one, the difference is that the external shape of the honeycomb has been made round on its extremity. A radius of 500 mm has been used, see Figure 3.7. The model was made up of 144429 nodes and 132930 elements: 95,3% brick elements

(35kg for the honeycomb) and 4,7% shell elements (61kg for the steel plates). The total mass of this model was 96kg.

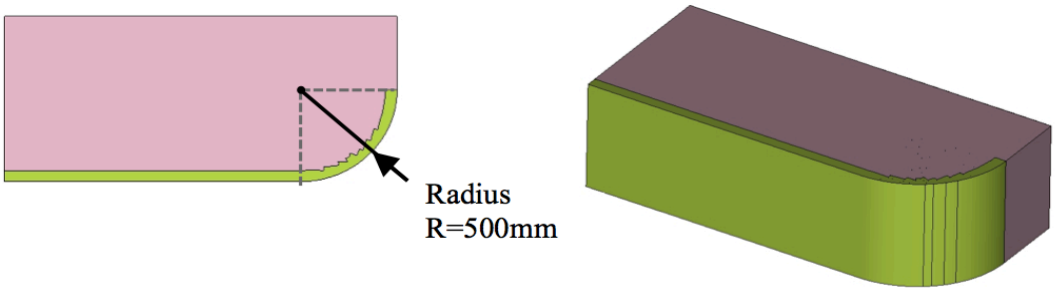

Figure 3.7 Honeycomb crash nose model with the round external shape

For the last new model, the front part has not been changed but the support structure has been bent with an angle of 45° at its extremity, see Figure 3.8. The model was made up of 63891 nodes and 64800 elements: 91% brick elements (17kg for the honeycomb) and 9% shell elements (54kg for the steel plates). The total mass of this model was 71kg.

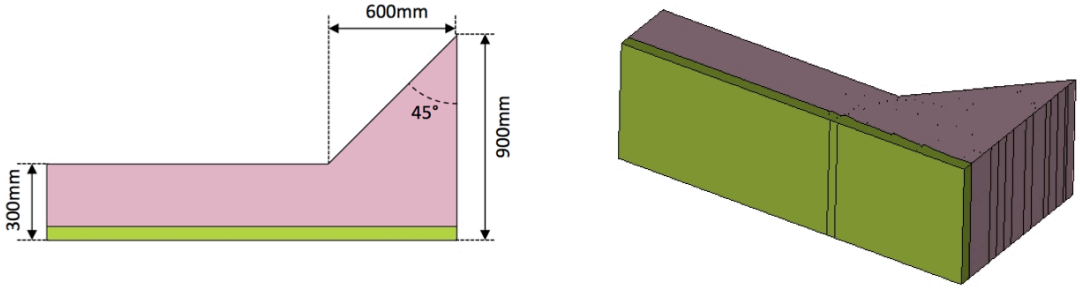

Figure 3.8 Honeycomb crash nose model with the angled support structure

- **"Lighter car model"**

The "lighter car model" has been created from the Volvo S80 model, only physical parameters have been modified (weight and front structure stiffness. Therefore, the number of structural elements is the same as the S80 model.

The final weight of this model was 1448kg and the thickness of the front structure elements has been reduced by 45% from the S80 model in order to have a front structure stiffness matching with the weight of this model.

3.2.3 Simplified truck model

For this simplified model, the truck has been simplified using a single mass of 12 tonnes placed at the truck center of gravity. A rigid body has been created between the honeycomb structure and this mass representing the truck, see Figure 3.9.

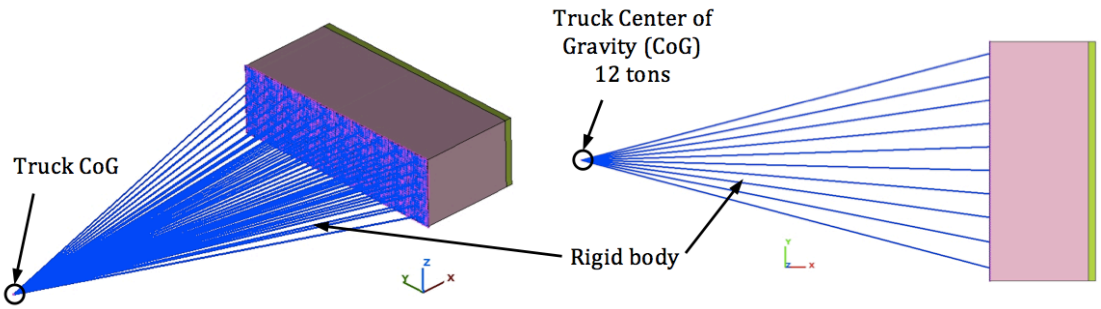

Figure 3.9 Simplified truck model (isometric and top view)

As for the truck models described Section 3.2.1, the mass representing the truck could be set up to be fixed or able to move backward. Even if the truck weight is much higher than the car, when the crash velocity is increased, the transfer of energy to the truck resulting in a movement backward cannot be neglected and therefore the rigid body needs to be able to move to give the same behaviour as the truck.

The use of this simplified model has been validated by comparing the results of different simulations from this model to those from the model with the truck. This validation has been done by comparing the car deformations, the repartition of the energy absorption between the truck nose and the car and the occupant load criterion to validate the simplified model.

3.3 Finite Element simulations

3.3.1 Reference load cases

In order to quantify the improvement due to the extended truck nose, the simulation results with the truck nose have been compared to different reference load cases. These reference load cases can be divided in two different groups: car-to-barrier simulations and car-to-truck.

Three different crash configurations have been used for the car-to-barrier crash.

- a full frontal crash in a rigid wall at 56 km/h that is the crash configuration used for the US-NCAP certification.
- a crash into a rigid wall with a horizontal overlap of 40% and with a closing speed of 56 km/h. This configuration should be fairly identical, in terms of energy absorption, to the EU-NCAP one which is a 40% overlap crash into a deformable barrier at a speed of 64 km/h.
- a rigid wall that has the same section dimensions than the honeycomb barrier used in the simplified model described in Section 3.2.3 and with a closing speed of 75 km/h.

Add to this, car-to-truck reference load cases have been used with two different truck models. For the first load case, the truck has been defined as a rigid body that means it would not get deformed while crashing. In the second load case the truck model was set up as deformable. This configuration should be more similar to a real car-to-truck collision than the non-deformable truck model. For both these two truck models, the crash configuration was the same that for the truck nose optimisation, that is to say head-on collision with a horizontal overlap of 75% of the car (around 57% of the truck). Different closing speeds have been used in order to compare with the different optimisation simulations.

3.3.2 Car-to-Truck simulations

In order to be able to improve the car to truck compatibility, it was important to better understand the behaviour of the car deformations experiencing a head-on collision with a truck. Therefore, it has been decided to investigate the differences that would appear between the car crashing into a rigid truck or into a flexible truck.

For this part, several simulations have been run using different parameters listed below:

- The truck was either flexible, that means that it could be deformed during the crash, or the truck was rigid and therefore not deformed during the crash
- Also, the truck was in some cases free to be pushed backward by the car during the crash, simulating a 12 tonnes truck. In other simulations, the rear of the truck has been fixed in order to simulate a infinitely loaded truck since it was restrained from behind
- Different horizontal overlaps have been used (from 25% to 66% of the car)
- Two impact speeds have been used: 56 km/h and 65 km/h

Then, when the additional truck frontal structure has been added to the truck, different simulations have also been done using the rigid truck for the first one and the flexible truck for the second with different overlaps and closing speeds. The analysis of these simulations aims to point out the importance of having a good support of the honeycomb structure.

3.4 Crash severity quantification

The improvements between the basic truck model and the ones with the new crash nose have been characterised by looking at different parameters. The crash severity (and occupant protection level) results in two main parameters: the geometric deformations of the car and the deceleration submitted to the occupants.

3.4.1 Car geometric deformations

In fact, the deformation of the safety compartment of the car can lead to severe injuries. Therefore, for each model, the effect on the geometry of the car has been analysed and two different geometrical parameters have been inspected.

The first one is the displacement of the A-pillar. Since this is where the dash panel is attached, any displacement of the A-pillar leads to a displacement of the instrument panel which reduces the survival space for the occupants. To get this parameter value, the relative displacement between a bracket fixed to the A-pillar and the middle of the car (assumed to be not deformed) has been extracted from the results, see Figure 3.10.

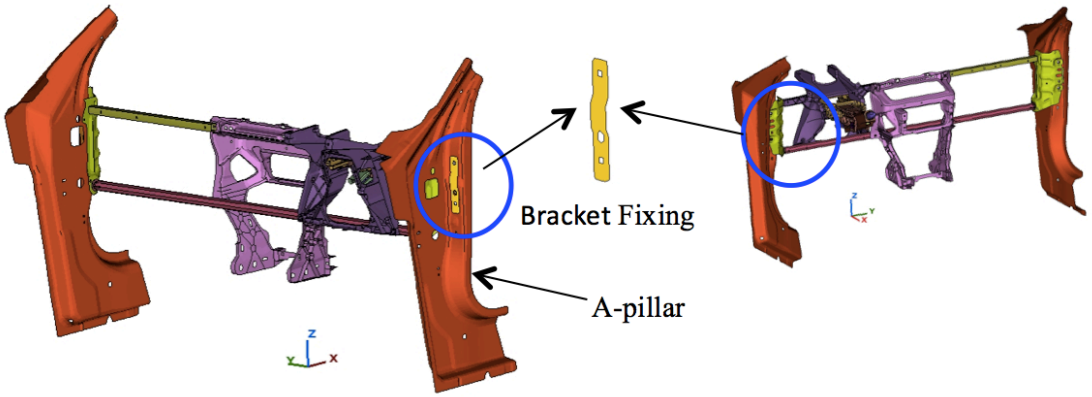

Figure 3.10 Location of the bracket used for the A-pillar displacement measures

The second geometrical parameter is the deformation of the car firewall (zone behind the instrument panel and pedals) that is also directly linked to the occupant compartment deformation. Fringe contour plots of these deformations have been used to show the improvements.

3.4.2 Occupant Load Criterion

Concerning the physical parameters, the car models used were not equipped with Hybrid III dummy models therefore direct improvements on occupant injury protection could not be seen but the deceleration submitted to the occupant seat also known as crash pulse has been analysed.

In crash severity characterisation, different crash pulse criteria are used either based directly on the pulses (e.g. maximum acceleration, point in time when the vehicle velocity is zero, velocity difference, average acceleration), or calculated from simplified mechanical models (e.g. Occupant Load Criterion (OLC) or Frontal Crash Criterion (FCC)) [20].

For this study, it has been decided to use an OLC that is based on the restrain force applied to the occupant chest. This criterion is based on a single mass model that is representing the occupant. This mass is linked to the car by a spring with a stiffness depending on the relative distance between the mass (occupant) and the car interior, see Figure 3.11.

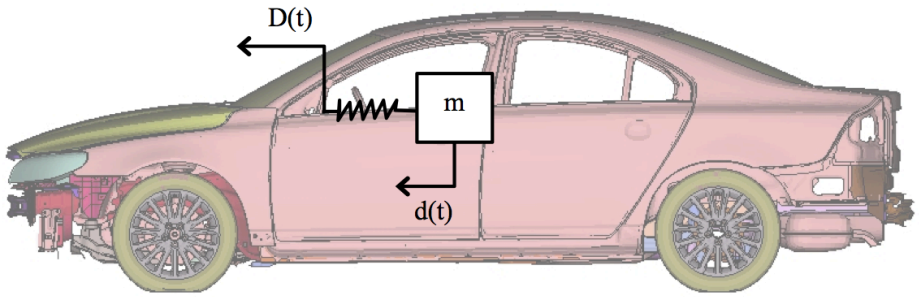

Figure 3.11 Schematic of the single mass model used for the OLC calculation.

For this model, X is defined as the relative distance between the mass (m=80kg) and the car therefore $X(t) = d(t) - D(t)$

At the beginning of the crash, the force on the occupant chest is very low (mainly because of the seatbelt slack distance), therefore for $0 < X < 65mm$, the restrain force F(X) is set up to zero. The mass representing the passenger is experiencing a free flight phase until a relative distance of 65 mm to the car is reached.

By integrating the momentum equation of the mass representing the occupant and using these initial conditions: $V(0)=V_0$= initial velocity of the car and d(0)=0, the following equations can be written (cst_1 and cst_2 are two constants):

$$m \cdot a(t) = F(X) = 0 \qquad (3.2)$$

$$v(t) = cst_1 = V_0 \qquad (3.3)$$

$$d(t) = V_0 \cdot t + cst_2 = V_0 \cdot t \qquad (3.4)$$

Once this relative distance of 65 mm is reached, the assumption is made that the occupant is ideally restrained. This is represented in the model by a constant spring stiffness resulting in a constant restrain force F_0 and so a constant deceleration of the occupant. The time at which this restrain phase starts is called t_0. This restrain force is applied until the relative distance between the occupant and the car reaches 300 mm, that time is called t_1. The restrain spring force characteristic is shown on the graph below.

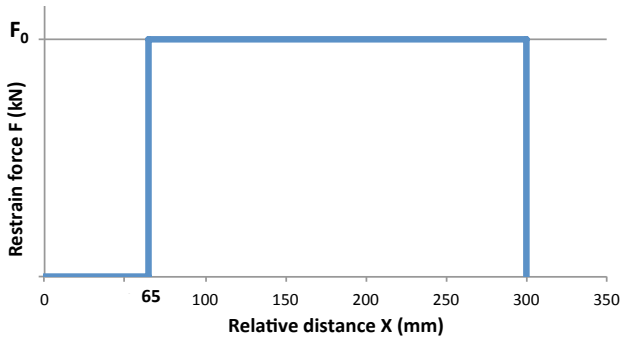

Figure 3.12 Restrain spring force characteristic used in the OLC model

For this second phase, the momentum equation is integrating again but the initial conditions are different: $F(X)=F_0$, $V(t_0)=V_0$ and $d(t_0)=d_0=D(t_0)$. Also, $T=t-t_0$ and cst_3 and cst_4 are two constants.

$$m \cdot a(t) = F(X) = F_0 \qquad (3.5)$$

$$v(T) = \frac{F_0 \cdot T}{m} + cst_3 = \frac{F_0 \cdot T}{m} + V_0 \qquad (3.6)$$

$$d(T) = \frac{F_0 \cdot T^2}{2 \cdot m} + V_0 \cdot T + cst_4 = \frac{F_0 \cdot T^2}{2 \cdot m} + V_0 \cdot T + d_0 \qquad (3.7)$$

According to equations (3.4) and (3.7) the displacement of the mass can be known, its velocity and acceleration also. An example can be seen Figure 3.13.

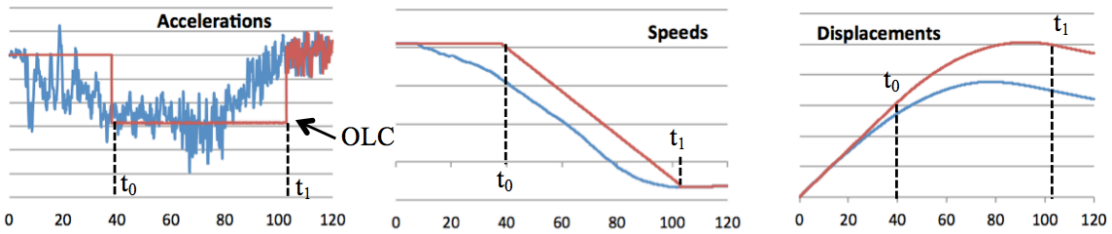

Figure 3.13 Acceleration, velocity and displacement time history of the vehicle (blue) and the occupant (red)

To determine the OLC value, the restrain force F_0 needs to be adjusted in order that the maximum relative distance between the mass and the car doesn't exceed 300 mm. Once this restrain force is found, the resulting constant deceleration value is the OLC value expressed in g's.

Once the OLC values are known, the results can be visualised in a plot function of the maximum displacement of the car D(t). A sample of OLC values for 440 different car models from 2000 to 2010 calculated from the US-NCAP 56 km/h rigid wall crash test can be seen Figure 3.14. The average OLC value for this sample is 30,5g.

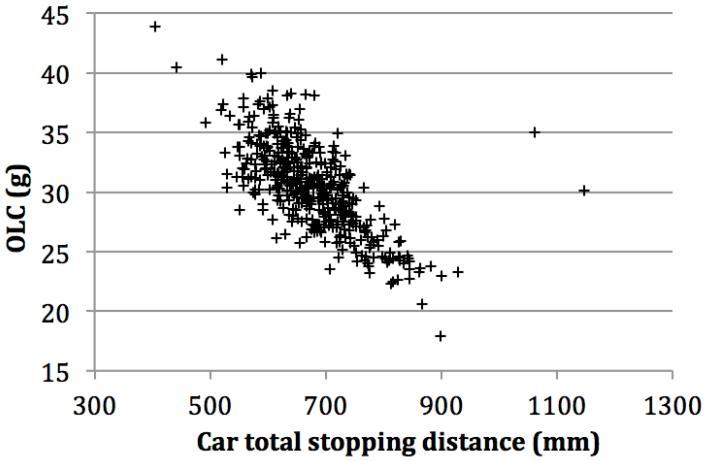

Figure 3.14 Sample of OLC values for 440 different car models from 2000 to 2010 calculated from the US-NCAP FF35 crash test (provided by VCC)

3.5 Additional truck frontal structure development

3.5.1 Load case and fixed parameters

For this study, some geometrical parameters have been fixed in order to reduce the numbers of variable parameters to make the optimisation easier. The effects of some of these parameters on the truck nose efficiency have been checked in the robustness checking but a further optimisation depending on these parameters could be the subject of a deeper study and optimisation.

The load case that has been used for the optimisation was a head-on collision between the truck and the car (impact angle equal to 0°) and with a horizontal overlap of the car of 75%, which represents around 57% of the truck, see Figure 3.15. Also, only the

model of the Volvo S80 was used for the optimisation and the lighter car model has been used later for the robustness checking.

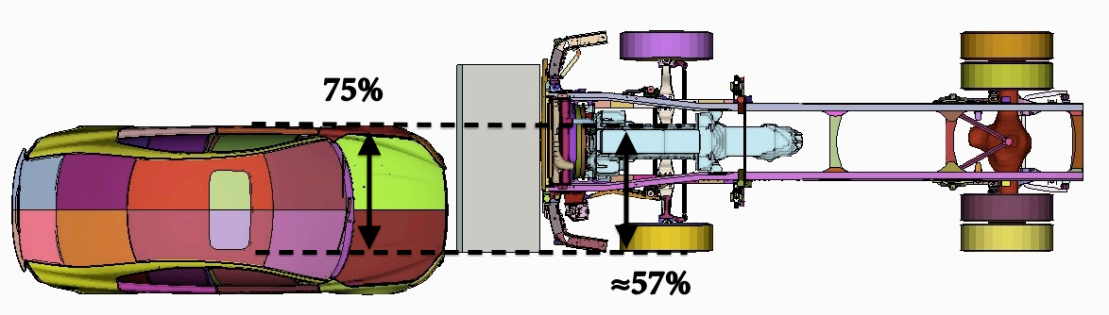

Figure 3.15 Load case overlap schematic

For the truck nose optimisation, the bumper heights above ground have been fixed in order to have a geometrical compliance between the car bumper and the truck frontal structure. Add to this, the ground clearance of the honeycomb crash nose is fixed to 200 mm in order to match with the car sub-frame of the Volvo S80, see Figure 3.16.

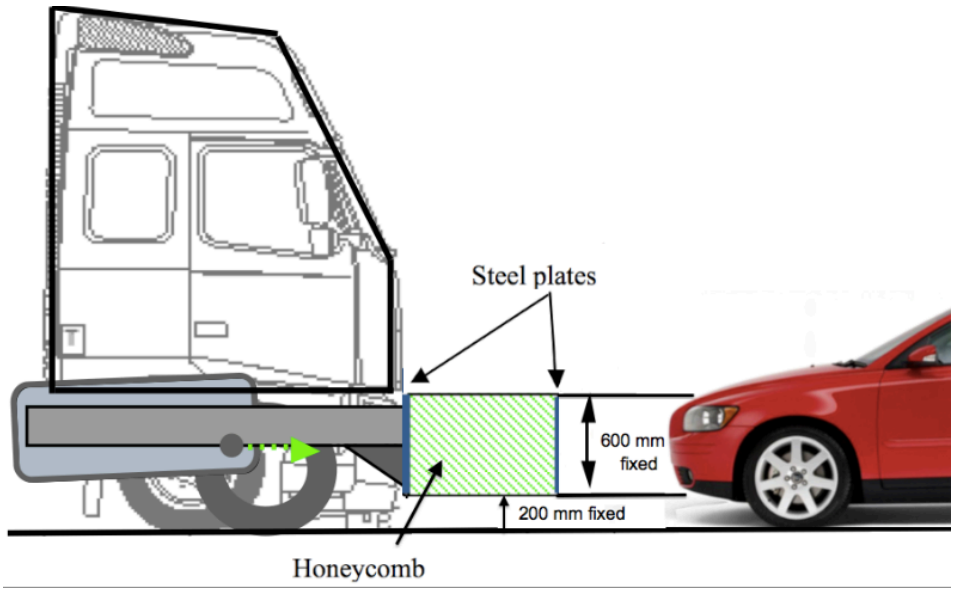

Figure 3.16 Load case bumper height. Side view

The front nose section height has also been fixed to 600 mm, see Figure 3.16. This height has been defined for the crash nose to catch the whole front structure of the car including the hood. Once again this parameter could be change in the shape design phase of the truck nose but it has not been done in this study.

3.5.2 Additional crash nose parameter study

This is why this study has been done using three different nose lengths from 300 mm up to 900 mm using steps of 300 mm. The first length studied was 900 mm because it is the length that seems to have the most benefits.

For all of these different lengths the crash nose has been optimised using the following methodology.

First, the model is run with a constant initial car speed and the honeycomb material properties are scaled in order to change the truck nose stiffness and therefore the force needed to crush it. The stiffness is optimised in order that the crash nose energy absorption is maximized for this specific initial car speed.

Once this optimised crash nose stiffness is found for that specific initial car speed, more simulations are run with different initial car speeds, using the optimised nose stiffness. For each nose length, the stiffness of the honeycomb structure has been optimised for four different car initial speeds (65,75,85 and 95 km/h).

3.5.3 Influence of the truck frontal crash structure shape

Once the basic truck crash nose stiffness has been optimised, it has been decided to look at the influence of having a different shape of the crash nose. Therefore, two different new models have been used. The first has been designed with an external round shape at its extremity, and the second has been shaped with a bent support structure, see detailed description Section 3.2.2.

- **Round external shape**

The purpose of this model was to investigate how does the external shape of the crash frontal structure affect the behaviour of the car while crashing into it in terms of crash severity but also general displacement of the car after the crash.

With that model, six simulations have been made using a unique closing speed of 75 km/h but different horizontal overlaps from 25 to 87,5% of the car.

- **Angled back plate**

This second model has been designed in order to see if by having the back support plate with an angle it would generate a glance off effect of the car. The aims of this angle is to try to make the car sliding on it and therefore, by changing the path of the car, to move the car out from the truck front. This was based on the idea that the small overlap crash severity (below 50%) could be decreased if the car path is changed.

This model has also been used for the simulations of crashes with a closing speed of 75 km/h and six different overlaps from 25 to 87,5%.

3.5.4 Robustness checking

Also, after the optimal stiffness of the crash nose has been found a robustness checking of the design had to be done to see that the crash front nose is also efficient for other impact scenarios than the nominal one used in the optimisation.

It has been decided to do this robustness checking using the 900 mm honeycomb structure with its stiffness optimised for an impact speed of 75 km/h.

This robustness checking has consisted in two different new sets of simulations. The first part was about running new impact scenarios for the Volvo S80 model. For this new configuration, the initial impact angle has been changed from a straight frontal collision to an angled collision with an impact angled of 12,5° and an overlap of 75%, see Figure 3.17. This load case has been run for the flexible truck model and for the simplified honeycomb structure, in both cases, the impact speed was 75 km/h and the rear of the truck was fixed.

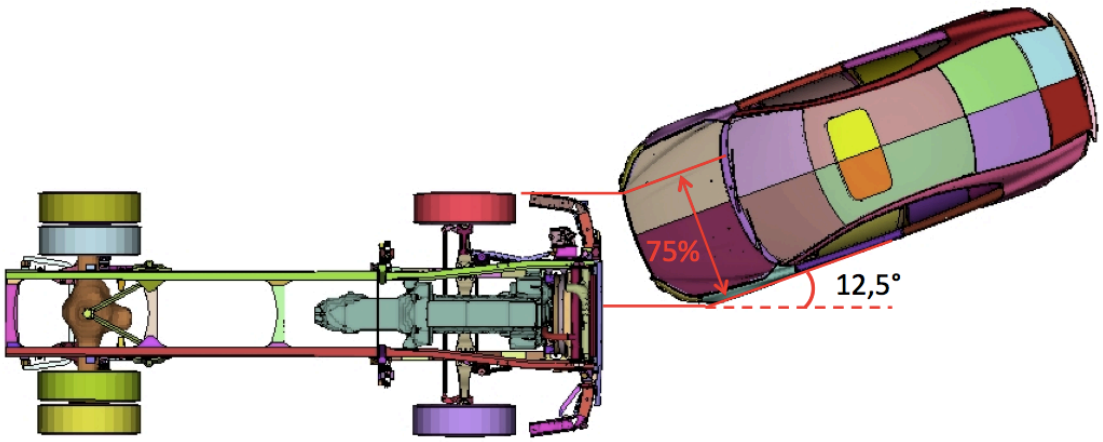

Figure 3.17 Angled impact load case schematic

The second part was about running the simulations with the lighter car model that has been created before, see Section 3.2.2. By these simulations, the aim is to check that the new front structure is also efficient for a lighter car for which the front stiffness is lower therefore the truck nose stiffness needs to be even lower in order to be deformed by a lighter car. Once again, the simulations have been run for the flexible truck model and for the simplified honeycomb structure described above. For this load case, three different impact speeds have been used for the simulations (56, 65 and 75 km/h).

4 Results

4.1 Optimisation of the honeycomb material stiffness

4.1.1 Validation of the simplified truck model

The following results show the comparison between the simplified truck model described Section 3.2.3 and the one with the honeycomb structure mounted on the Rigid Heavy Truck (RHT) described Section 3.2.1. The simulations performed were representing a frontal crash with 75% horizontal overlap and a closing speed of the car from 65 to 95 km/h. The honeycomb structure used was the 900 mm-length with its stiffness optimised for 75km/h. Simulations #1 and #2, see Appendix 8.2.

- **Comparison of the car deformations**

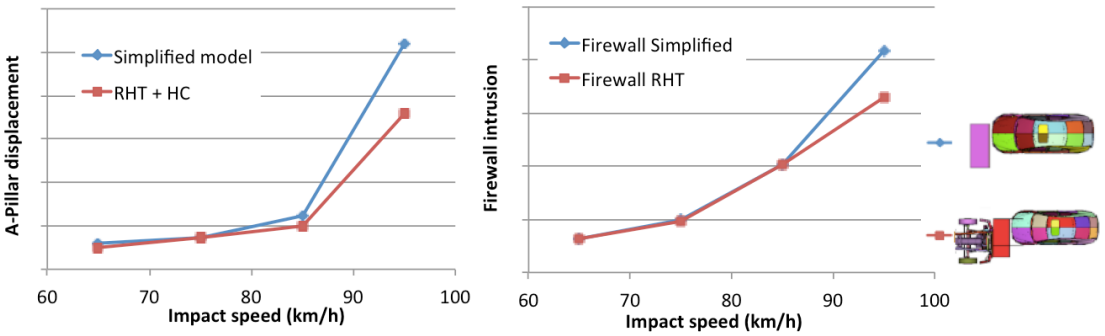

Figure 4.1 Car deformations in respect of the impact speed. Left: A-pillar displacement; Right: Firewall intrusion

Figure 4.1 shows that the A-pillar displacement and the firewall intrusion given by both models are really similar up to an impact speed of 85 km/h. When the closing speed is increased to 95 km/h, the results follow the same trend but the one from the simplified model are 25% higher for the firewall intrusion and 44% higher for the A-pillar displacement.

- **Comparison of the energy absorption repartition**

The following graphs show the comparison of the repartition of the energy absorption between the car and the honeycomb structure using the two different models. The Figure 4.2 shows for one load case the details of the energy absorption distributions during the crash. The different energies plotted are the one absorbed by the honeycomb, the one absorbed by the car and the total deformation energy. This comparison has been done for the four closing speeds and the sum up can be seen on Figure 4.3.

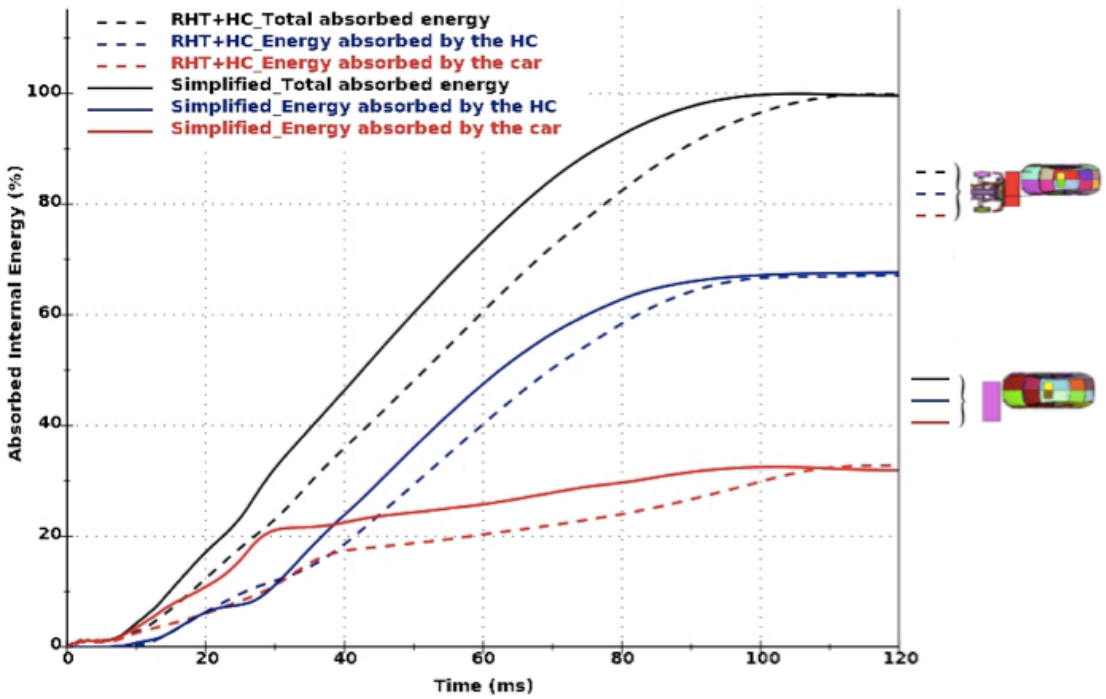

Figure 4.2 Comparison of the energy absorption for the RHT and the simplified models. 75% overlap crash at 65 km/h with the 900 mm honeycomb structure

One can see that even though the energy absorption curves are slightly different between the two truck models, the final repartition is similar. This is mostly the same also for the other closing speeds as it can be seen in Figure 4.3.

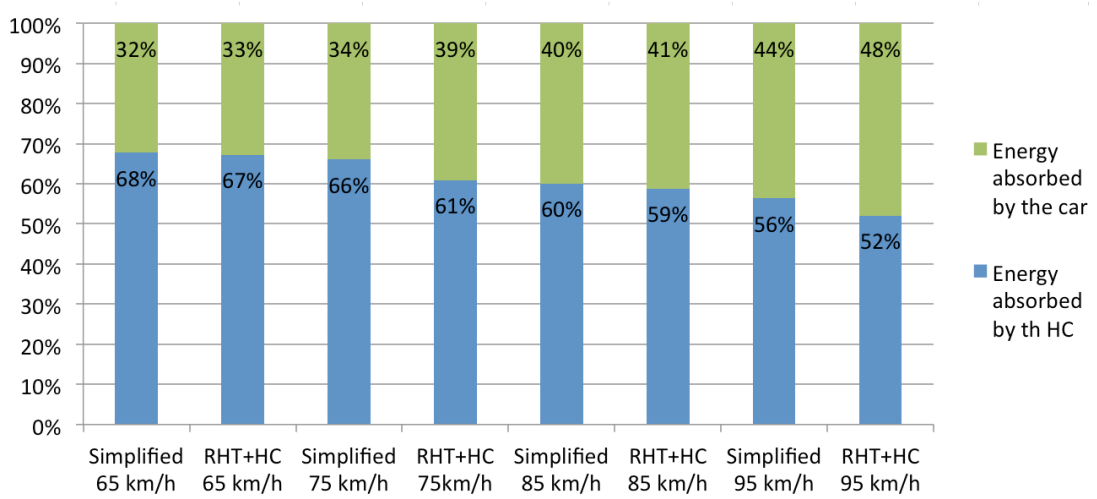

Figure 4.3 Repartition of the energy absorption between the car and the HC

- **Comparison of the OLC**

The last criterion that has been used to compare the two models was the OLC. The following graph shows the OLC values as a function of the closing speed for the two models. It can be seen that for the simplified model, the OLC values are higher by an average of 16,5% compared to the RHT model, see Figure 4.4. The higher OLC values from the simplified model can be explained by a different displacement of the truck for the two models during the crash due to a different weight distribution for the simplified model.

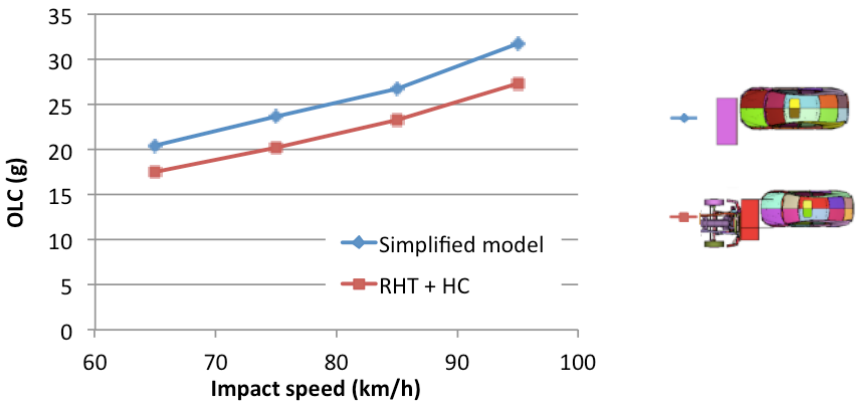

Figure 4.4 OLC values as a function of impact speed

This difference between the to models has been considered to be acceptable for the results since the OLC values calculated from the simplified model are higher that means that there are maximized compared to the normal model.

4.1.2 Optimisation of the honeycomb material stiffness

According to the material specification [18], the crush strength limit for the main honeycomb material is set to 0,310MPa and 1,690MPa for the bumper honeycomb material.

In the case of our simulations, this crush strength has been calculated from a simplified model of the honeycomb structure of 900 mm and an impact speed of 75 km/h. The simulation has been run for different yield strength factors of the main honeycomb material as they have been scaled for the honeycomb stiffness optimisation. The crush strength has been calculated by divided the impact force by the surface of the deformed honeycomb section. The honeycomb crush strength for various scale factors can be seen Figure 4.5.

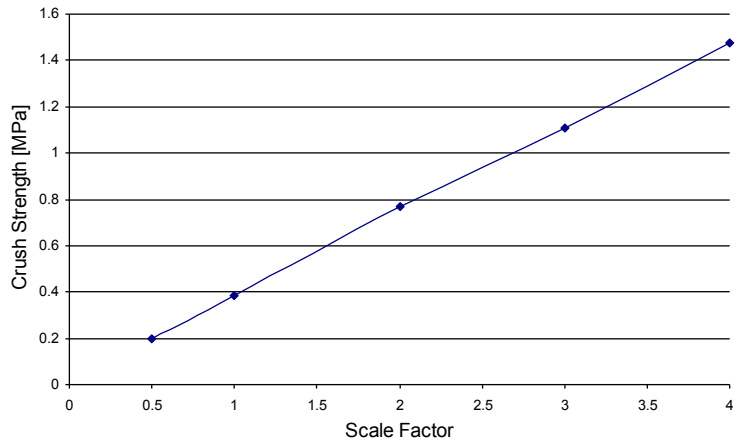

Figure 4.5 Crush strength vs Scale factor for the main honeycomb material

From these results, the main honeycomb block crush strength was 0,385MPa, this value was set as the reference point for the optimisation.

In order to obtain the optimal stiffness for each honeycomb structure length previously defined 300, 600 and 900 mm and a set speeds of 65, 75, 85 and 95 km/h

(simulations #3, see Appendix 8.2), it was decided to scale the yield strength factors of the main honeycomb material. The optimal honeycomb stiffness was considered when the maximum energy absorption from the honeycomb structure was reached. The graph below shows the distribution of the energy absorption of the car and the honeycomb structure for one load case (75 km/h and 900 mm honeycomb structure).

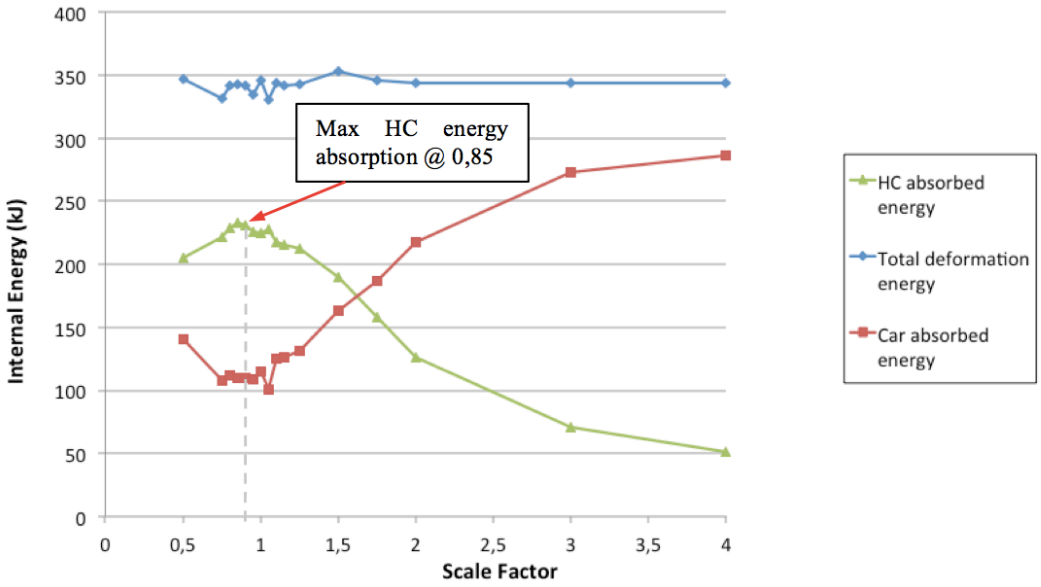

Figure 4.6 Optimisation for 900 mm-length honeycomb (HC) structure at 75 km/h

Once the optimal value for each speed has been calculated, the same material stiffness was used to run the simulation for the different impact speeds. Then the maximum energy absorbed by the honeycomb has been extracted from these simulations. The results are shown in the Table 4.7.

	HC Energy Absorption [kJ]				HC Energy Absorption [kJ]				HC Energy Absorption [kJ]			
	300 [mm]				600 [mm]				900 [mm]			
Test Velocity / Optimized Velocity	65 [km/h]	75 [km/h]	85 [km/h]	95 [km/h]	65 [km/h]	75 [km/h]	85 [km/h]	95 [km/h]	65 [km/h]	75 [km/h]	85 [km/h]	95 [km/h]
65 [km/h]	**96**	117	136	157	**155**	182	214	247	**183**	222	265	336
75 [km/h]	95	**118**	136	164	153	**184**	219	255	179	**233**	269	320
85 [km/h]	96	117	**144**	168	145	180	**223**	262	172	226	**275**	328
95 [km/h]	90	115	141	**169**	135	179	217	**265**	172	226	275	**328**

Table 4.7 Honeycomb energy absorption for 300, 600 and 900 mm crash nose

It can be seen in Table 4.7 that the maximum energy absorption by the honeycomb for each test velocity corresponds to the one reached at its optimised velocity (bold values). The velocity use for the parameter study doesn't affect much the energy absorption compared to the length of the honeycomb structure.

The optimal stiffness for each configuration has been calculated in terms of crush strength with the respective maximum energy absorption, see Figure 4.8.

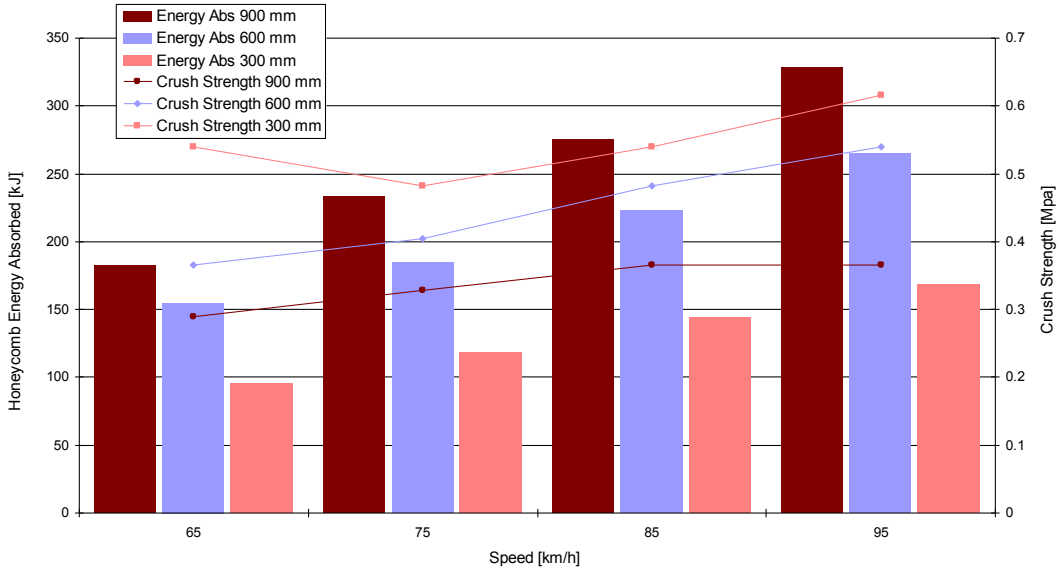

Figure 4.8 Energy absorption and optimised HC crush strength for 300, 600, 900 mm and 65, 75, 85 and 95 km/h

It can be seen Figure 4.8 that the optimised crush strengths for the 900 mm-length structure are between 0,288MPa and 0,365MPa but for the shorter structures, this crush strengths are higher (e.g. up to 0,620MPa for the 300 mm-length honeycomb structure optimised for an impact speed of 95 km/h).

The influence of these higher values is that the force needed to deform the honeycomb material increases, see Figure 4.9. The beginning of the honeycomb deformation starts around a displacement of the car of 400 mm (green dashed line). It can be seen that initially, the forces are quite close between 325kN and 425kN. Then, at the end of the honeycomb structure deformation (red dot), the difference is much higher for the three different structure lengths, respectively 425kN, 600kN and 800kN. If the honeycomb crush force is too high compared to the front structure stiffness of a lighter car for instance, the car will be deformed before the honeycomb material.

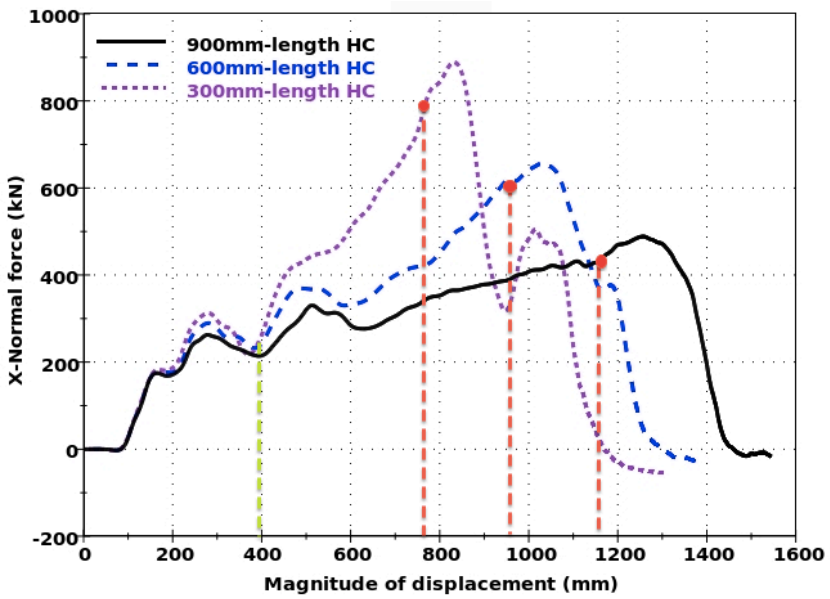

Figure 4.9 Force-displacement curves for three crash nose lengths optimised for an impact at 75 km/h. (75% horizontal overlap & 75 km/h)

4.1.3 Improvement due to the 900 mm-length honeycomb structure

One effective way of comparing the infinitely loaded state (FHT fixed) to the addition of a 900 mm-length honeycomb structure (HC), is to measure the A-pillar displacement, the firewall intrusion and compare the OLC. The honeycomb structure used for these load cases is the one optimised for a closing speed of 75 km/h. Simulations #4 and #5, see Appendix 8.2.

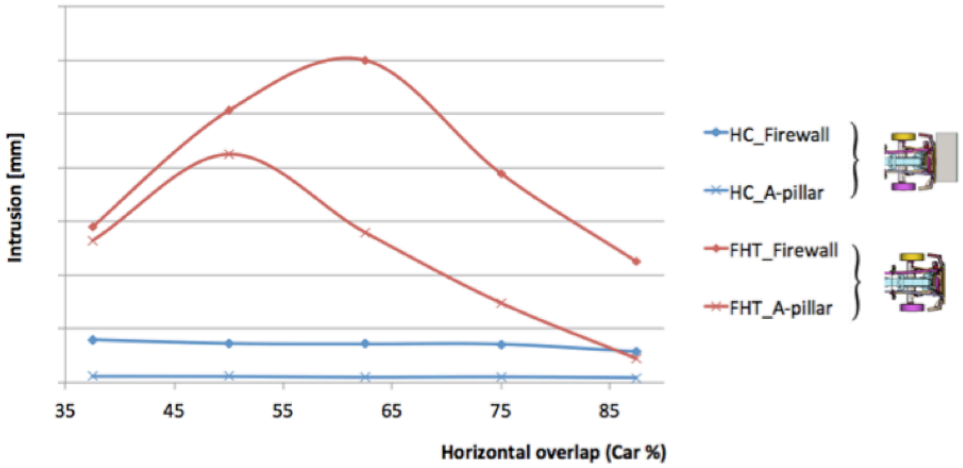

Figure 4.10 Intrusion into the firewall and A-pillar displacement as a function of the horizontal overlap with a closing speed of 65km/h.

As it can be seen Figure 4.10, with the honeycomb structure, the car deformations are much lower compared to the FHT. With the honeycomb structure, the A-pillar and firewall intrusions were below 50 mm for a closing speed of 65 km/h.

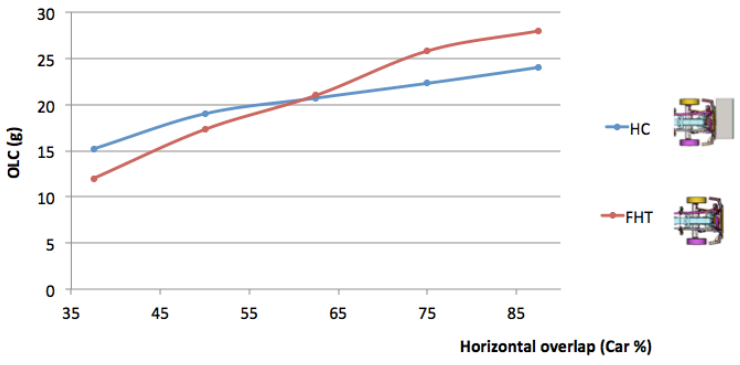

Figure 4.11 OLC values as a function of the overlap at 65km/h

With the honeycomb structure, a reduction of the OLC was seen for overlaps above 62,5% while a slight increment for 50 and 37,5% overlaps, see Figure 4.11. The fact that higher OLC values for the simplified honeycomb model were observed, can be explained since there was not any deformation of the truck compared to the FHT. Because of the truck deformation, the stopping distance is increased and that leads to a lower deceleration pulse; i.e., lower OLC. On the other hand, for small overlaps, these truck deformations can enable the car to hit the truck front wheel since it doesn't stop it.

The Figure 4.12 shows the energy absorption repartition between the car and either the truck or the HC structure depending on the model. The simulation load case was a 75% overlap collision with a closing speed of 65 km/h and the two models compared are the FHT and the 900 mm-length HC structure.

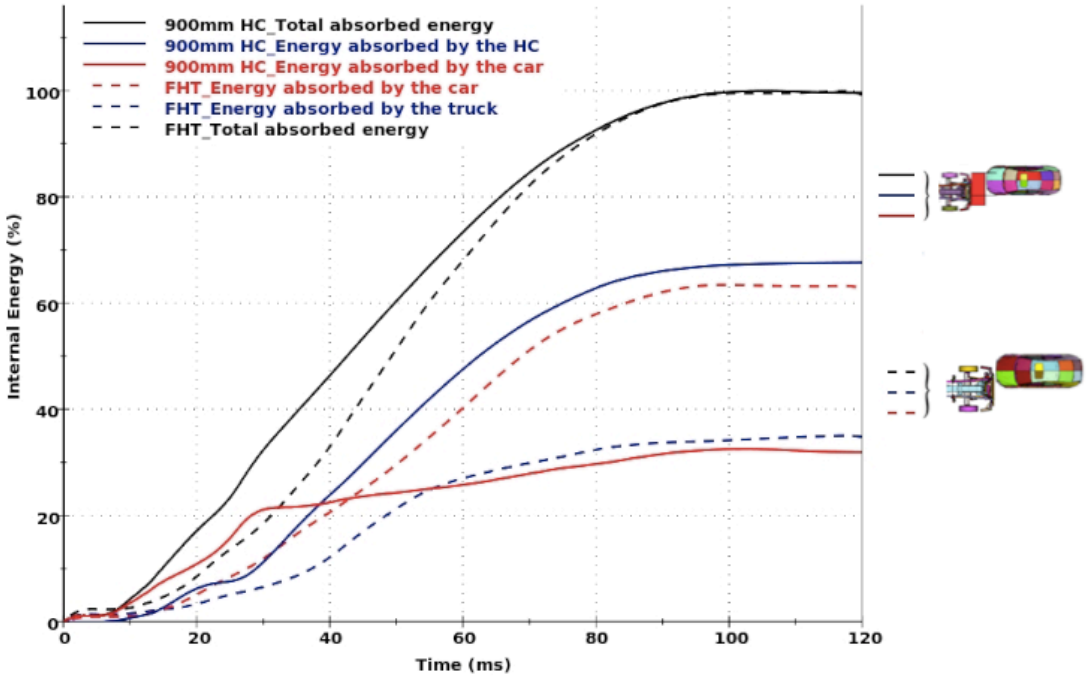

Figure 4.12 Energy absorption repartition for a 75% overlap collision at 65 km/h

The main difference that can be seen from this graph is that in case of the crash between the truck and the car (dashed line curves), the energy absorbed by the car represents 65% of the total deformation energy whereas using the HC structure (full line curves), the energy absorbed by the car is only 32% since 68% is absorbed by the HC structure. Lower energy absorption means lower deformation for the car.

4.2 Robustness checking of the optimised structure

From the results of the optimisation of the honeycomb material stiffness of the new truck frontal structure, it has been decided to do the robustness checking for one truck front structure model. For the following load cases, the honeycomb structure used was the 900 mm-length with its stiffness optimised for an impact speed of 75 km/h and the reference is the fixed flexible heavy truck.

4.2.1 Angled impact load case

The simulation results show that using the honeycomb structure is also efficient in case of angled impact of 12,5° with 75% horizontal overlap (simulations #6 and #7, see Appendix 8.2). By using the honeycomb front structure, the maximum displacement of the A-pillar is decreased by 73% and the firewall intrusion is lowered by 66%. On the other hand, the OLC is increased by 8%, rising to 29,8g with the honeycomb compared to 27,6g without the honeycomb since the truck deformation increases the deformation length compared to the rigid support structure.

4.2.2 Impact with a lighter car

For the simulations with the lighter car model, three different impact speeds have been used 56, 65 and 75 km/h (simulations #8 and #9, see Appendix 8.2). The table below shows the improved results from the additional frontal structure compared to the regular truck. Negative values stand for lower values and therefore improvements.

	56 km/h	65 km/h	75 km/h
A-Pillar displacement	- 69%	- 94%	- 97%
Firewall intrusion	- 4%	- 43%	- 87%
OLC	+ 2%	- 4%	- 4%

Table 4.13 Improvements from the honeycomb front structure using the lighter car model compared to the current truck

It can be seen the honeycomb structure is very efficient while looking at the car deformations without affecting that much the deceleration peak expressed through the OLC. As the speed increases, the results are becoming more and more important since the critical impact speed is reached. While looking at the car to truck crash, it can be seen that above 65 km/h, the car is seriously deformed, included the occupant compartment. This speed can be considered as the critical impact speed for this lighter car frontal crash to a truck.

4.3 Analytical calculations

From the simulation results of the Volvo S80 crashing into the rigid wall with an horizontal overlap of 75% with an impact speed of 75 km/h, the impact force has been extracted and the force-displacement curve has been plot, see Figure 4.14. From this curve, the maximum energy absorbed by the car has been approximated using the method explained in Section 3.1.

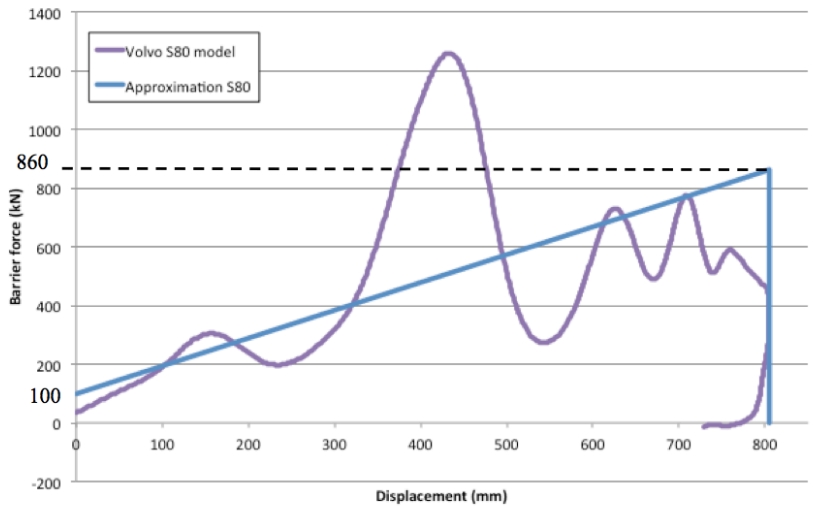

Figure 4.14 Force-Displacement curve from the simulation of the Volvo S80 crashing into a rigid wall, with 75% horizontal overlap and at 75 km/h

From this force-displacement characteristic, the car energy absorption has been calculated. For this load case, the car frontal structure deformation energy absorption has been estimated to be around 386kJ. From the post-processing analysis, the car energy absorption was 420kJ. The linear approximation method is, for this load case, not such accurate because of the force peak. Therefore the value that has been used was 420kJ.

This result is close to the one used in the study "*Safer aerodynamic frontal structures for trucks*" [5], in which they estimated the maximum energy absorption of a larger car (1700kg) to be 360kJ for a critical impact speed into a 12 tonne rigid truck of 79 km/h.

Now that the car maximum energy absorption has been estimated, the critical impact speeds have been calculated for the different truck frontal structure length and crushing force. The results are shown on the graph in Figure 4.15.

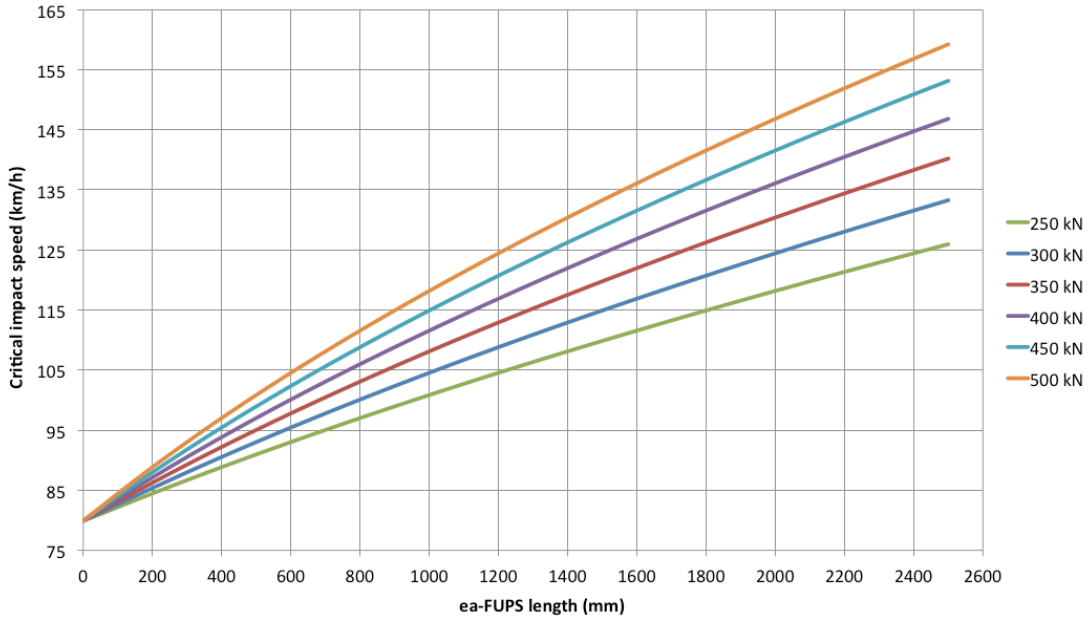

Figure 4.15 Critical (equivalent energy) impact speeds for different ea-FUPS crush length & force

The results show that using a constant crush force ea-FUPS, the Volvo S80 critical speeds could be raised from about 80 km/h up to about 125-160 km/h depending of the truck nose crush force and length. From the simulations, the critical impact speed without honeycomb structure was around a closing speed of 72 km/h for the current flexible truck and 77 km/h with the rigid truck. The critical speeds for the three specific lengths used in the truck frontal structure optimisation are shown in Table 4.16.

	Truck frontal structure length		
	300mm	600mm	900mm
Critical impact speed (depending on the ea-FUPS crush force)	from 88 to 93 km/h	from 93 to 104 km/h	from 99 to 115 km/h

Table 4.16 Critical speeds calculated from the analytical method

From the optimisation of the honeycomb structure results, the amount of energy that can be absorbed by the honeycomb has been estimated for the three different truck structure lengths, see Table 4.7. As it was estimated above, the maximum energy absorbed by the car deformation is 420kJ, therefore the maximum total deformation energy can be estimated (since it is the sum of the two) and the critical speeds from equation 3.1.

		Energy absorbed by the car deformation	Energy absorbed by the truck nose	Total deformation energy	Critical impact speed
Truck frontal structure length	300mm	420kJ	169kJ	589kJ	95 km/h
	600mm	420kJ	265kJ	685kJ	102 km/h
	900mm	420kJ	330kJ	750kJ	107 km/h

Table 4.17 Critical speeds from the simulation results

4.4 Importance of having a good back plate support

4.4.1 Comparison between flexible and rigid truck

- **Effect on the interaction between the car and the truck**

The simulations of the car crashing into the two different truck models have shown that the car behaviour is different whether the truck is flexible or rigid as well as the car deformations.

For the following results, the initial parameters were an impact speed of 65 km/h, with horizontal overlap of 50% of the truck, (simulations #10 to #13, see Appendix 8.2). The truck was either fixed by its rear, or being able to be pushed backward by the car during the crash. In Table 4.18, the rigid truck results are compared to the flexible truck that is the reference. Negative values stand for improvement.

	Moving truck	Fixed truck
A-Pillar displacement	- 69%	- 82%
Firewall intrusion	+ 1%	- 19%
OLC	+ 30%	+ 47%

Table 4.18 Comparison between flexible (reference) and rigid truck at 65 km/h with 50% horizontal overlap

The results above show the difference between the car crashing into the rigid truck compared to the flexible truck. It can be seen that the maximum displacement of the A-pillar is much lower when the truck is rigid. At the same time, the intrusion is the firewall is also lowered.

These lower deformations result in an increase of the OLC that goes up by nearly 50% when the rigid truck is fixed compared to the flexible one but it can be noticed that in the worse case while looking at the deceleration peak (rigid and fixed truck), the OLC is equal to 33g which is still an acceptable value compared to the average value from the US-NCAP that is 30,5g, see Figure 3.14.

The pictures below show that the firewall is also deformed differently between the crash in the rigid and flexible truck. The Figure 4.19 shows the firewall intrusion whereas the Figure 4.20 shows a side cut view at the firewall maximum deformation.

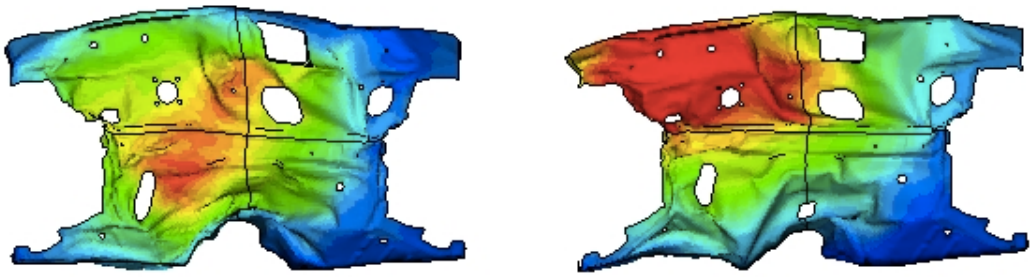

Figure 4.19 Maximum firewall intrusion (in red), the same colour scale is used for both cases. Left side: fixed rigid truck. Right side: fixed flexible truck

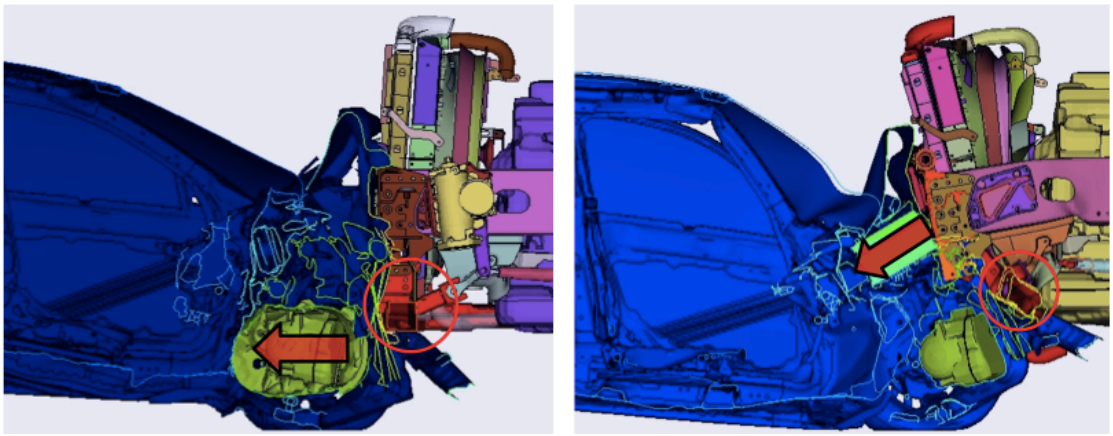

Figure 4.20 Cut side view when the firewall intrusion is maximum. Left side: fixed rigid truck. Right side: fixed flexible truck

It can be seen that for the flexible truck, Figure 4.20 right, the FUPS (red circle) is bent backward absorbing some energy but therefore the car side hits the truck frame beam that leads to the deformation of the upper left part of the firewall, see Figure 4.19.

In the case of the rigid truck Figure 4.20 left, since the FUPS (red circle) is now non-deformable, it catches the engine and gearbox of the car that explains the lower deformation in the car firewall, see Figure 4.19.

Therefore, even if the firewall intrusion doesn't change much between the crash with the rigid and with the flexible truck mainly for the moving load case, the deformation location is important. While deforming the firewall upper part, it leads to the intrusion of the steering column in the occupant compartment.

The behaviour of the car is also different after the crash. In the case of the flexible truck, the residual kinetic energy leads to a rotation of the car around the vertical axis whereas in the case of the rigid truck, the car has a tendency to rebound on the truck and move backward. In that second load case, the car rotation is much lower, see Figure 4.21.

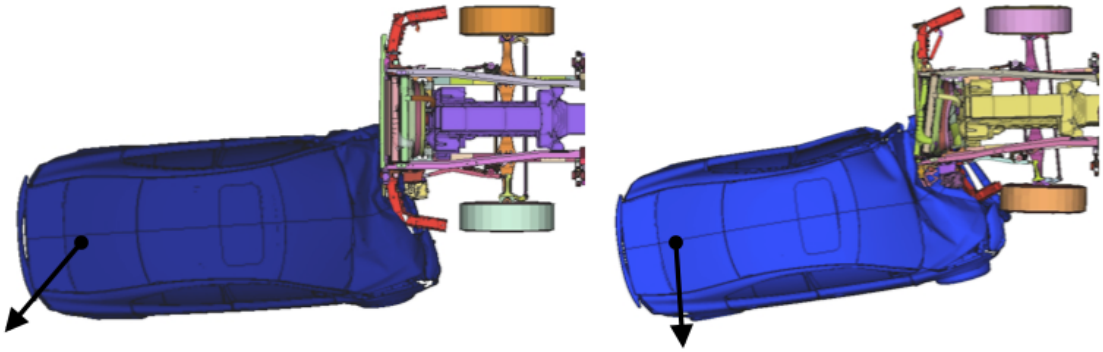

Figure 4.21 Direction of the car movement after the crash. Left side: fixed rigid truck. Right side: fixed flexible truck

- **Effect on the additional structure energy absorption**

The influence of the rigidity of the truck front has also been investigated with the additional honeycomb structure in the front of the truck (simulations #14 and #15, see Appendix 8.2). The amount of energy absorbed by the honeycomb structure is directly linked to its deformation. Now, in case of the deformable truck, once the honeycomb structure deformation begins, the truck front structure starts also to bend backward. Because of this deformation, the back plate of the honeycomb structure has not a good support and therefore it bends. This leads to a lower deformation of the additional structure, see Figure 4.22.

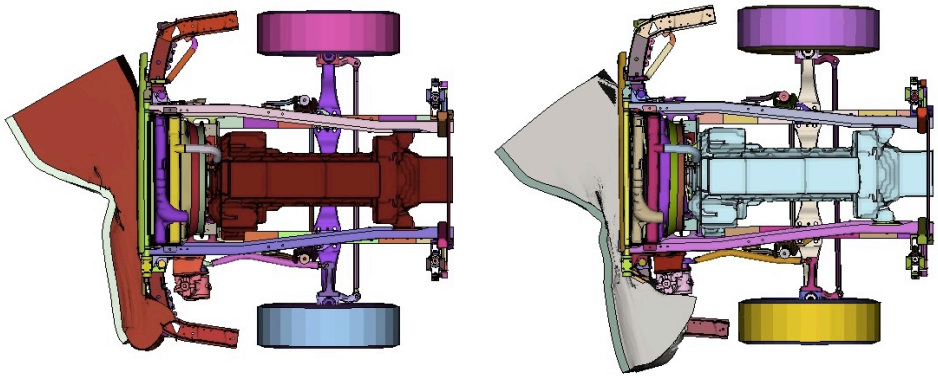

Figure 4.22 Maximum deformation of the honeycomb structure. Simulation of a head-on collision at 65 km/h with a horizontal overlap of 75% of the car. Left side: rigid truck. Right side: flexible truck

The effect of this lower deformation of the additional structure affects directly the amount of energy that it absorbs. The chart below shows the percentage of energy absorbed by the honeycomb structure for the flexible and rigid truck and different impact speeds, see Figure 4.23.

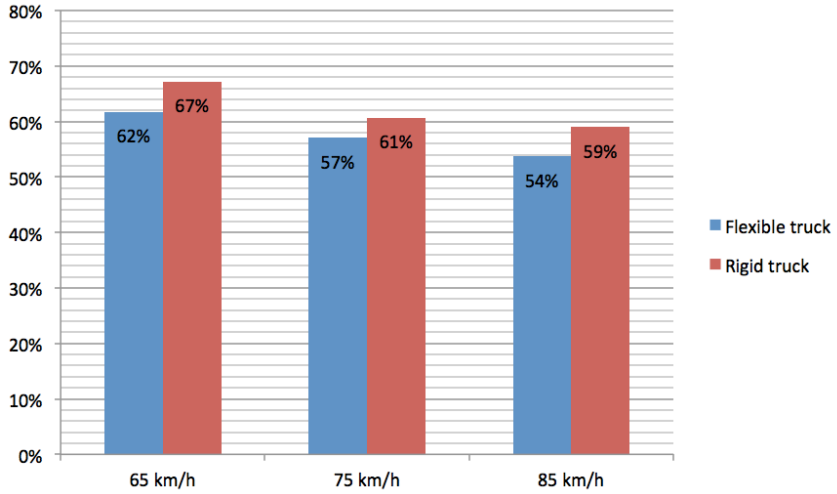

Figure 4.23 Honeycomb energy absorption for different impact speeds using both rigid (RHT) and flexible truck (FHT) with a 900 mm-length HC structure

These results show that when the honeycomb structure is fixed on front of the rigid truck, the proportion of energy that it absorbs is higher by an average of 5%. This confirms what has been said above that a better deformation of the honeycomb leads to higher energy absorption.

4.4.2 Small overlap head-on crashes with the flexible truck

- **Regular trucks without HC**

In case of head-on crash with small horizontal overlaps (25% and 37,5% of the car) using the flexible truck, an important phenomenon has appeared. Simulations #16, see Appendix 8.2.

While crashing, the car is only caught by the FUPS side extremity and its strength is not high enough to stop the car since the truck bumper gets bent. Because of this the car crashes into the front wheel of the truck, see Figure 4.24.

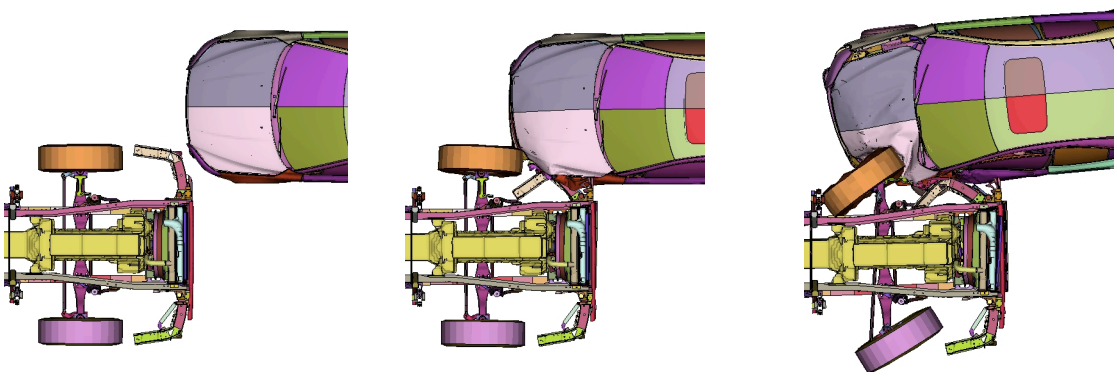

Figure 4.24 25% overlap head-on collision with the flexible truck at 65 km/h. Left: 5ms before impact; Middle: 50ms after impact; Right: 120ms after impact

The same phenomenon has been seen for a 37,5% horizontal overlap. This is a big issue since it leads to large car intrusions due to geometrical incompatibility. Also the car energy absorption is low since the deformable zone of the car is not fully engaged.

- **Trucks with HC structure**

This load case has also been investigated with the 900 mm-length honeycomb mounted on both the flexible and rigid truck. In both cases the truck rear was fixed. The crash configurations were 25% and 37,5% head-on collisions with a closing speed of 75 km/h. Simulations #17 and #18, see Appendix 8.2.

The comparison between the two different trucks with a 37,5% horizontal overlap crash is shown Figure 4.25 and Figure 4.26.

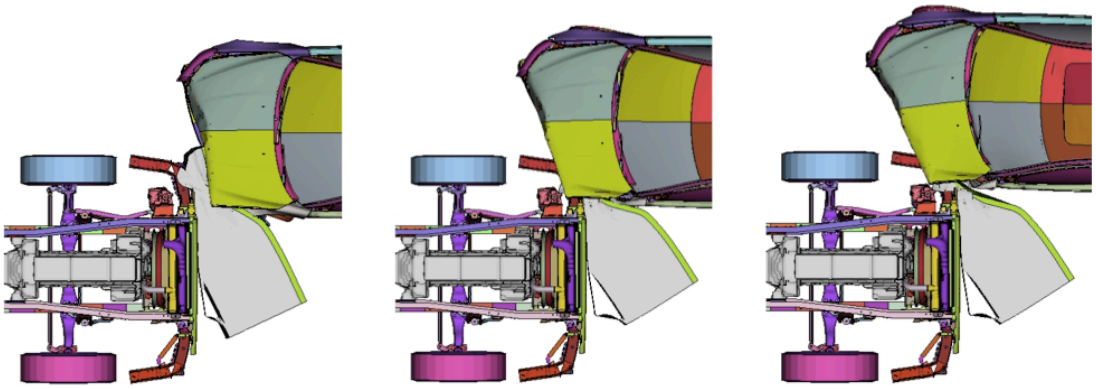

Figure 4.25 37,5% overlap head-on collision with the rigid truck at 75 km/h. Left: 65ms after impact; Middle: 100ms after impact; Right: 130ms after impact.

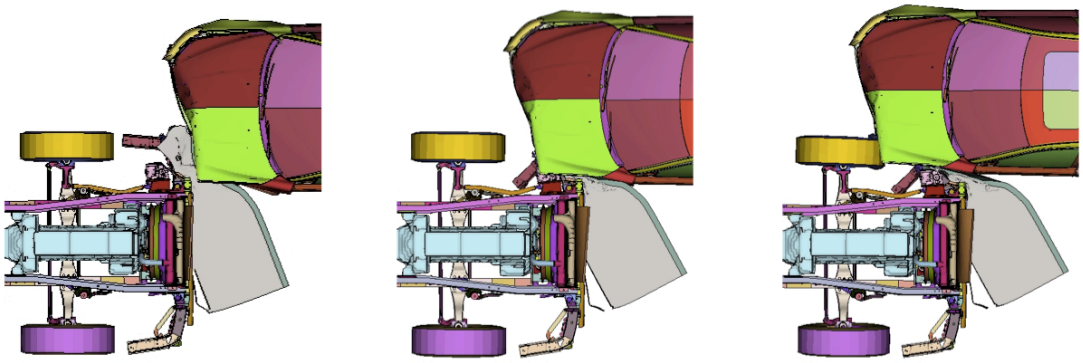

Figure 4.26 37,5% overlap head-on collision with the flexible truck at 75 km/h. Left: 65ms after impact; Middle: 100ms after impact; Right: 130ms after impact.

From the two figures above, the same results than without the honeycomb structure can be seen. When the truck is flexible, the FUPS bends behind the honeycomb structure since the stiffness of this part cannot handle the forces acting on it. The deformation of the FUPS leads to a higher energy absorption but the main issue is that the car is not stopped or deflected and therefore hits the truck front wheel in comparison to the rigid truck that prevents this collision between the car and the truck front wheel.

The comparison between the two different trucks with a 25% horizontal overlap crash is shown Figure 4.27 and Figure 4.28.

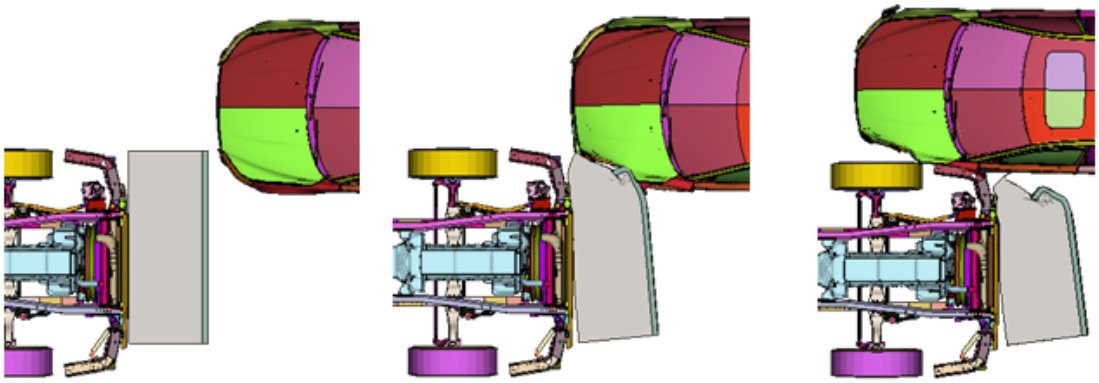

Figure 4.27 25% overlap head-on collision with the rigid truck at 75 km/h. Left: 5ms before impact; Middle: 60ms after impact; Right: 175ms after impact.

In the case of the rigid truck, it is possible to see a small deflection of the car due first to the honeycomb structure deformation and then to the fact that the truck bumper was not deformed and therefore the car is slightly deflected while hitting the truck bumper, see Figure 4.27.

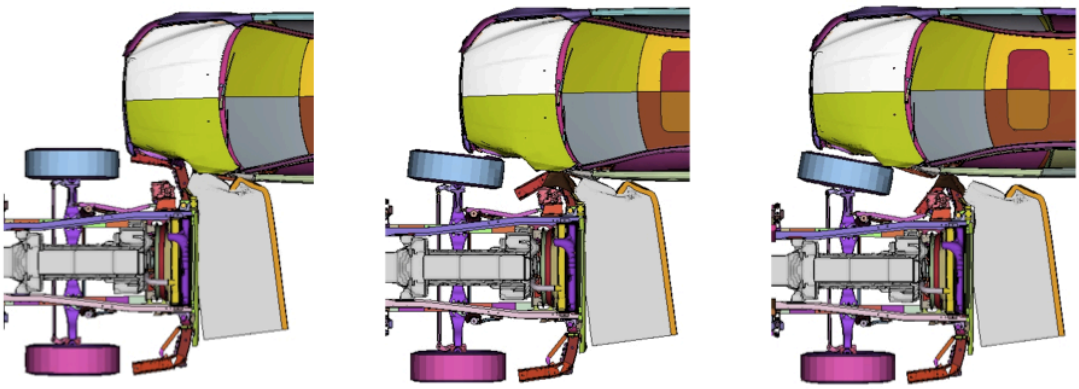

Figure 4.28 25% overlap head-on collision with the flexible truck at 75 km/h. Left: 90ms after impact; Middle: 120ms after impact; Right: 140ms after impact.

When the truck is flexible, it can once again be seen that because of the FUPS deformation, the car hits the truck front wheel whereas it is something that should be avoided.

4.5 Influence of the frontal structure shape

4.5.1 Back support plate shape

The importance of the back support plate shape in case of small overlap collisions was found to be a key factor in promoting a glancing off effect. The results from the two different back plate shapes are shown below. Simulations #19 and #20, see Appendix 8.2.

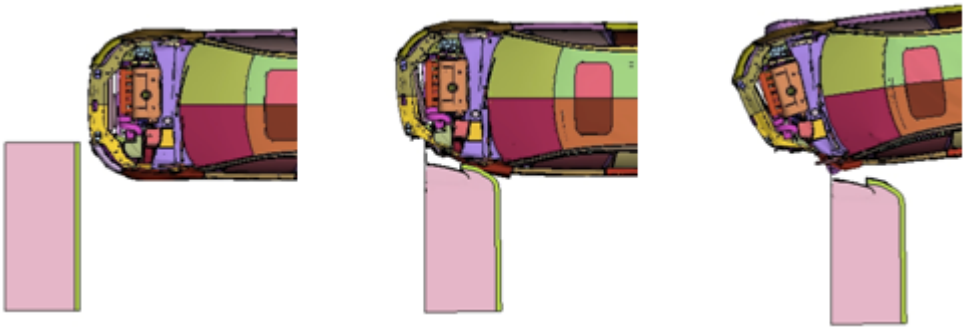

Figure 4.29 Simulation of a 25% overlap crash at 75 km/h with the straight support structure. Left: before impact; Middle: 65ms after impact; Right: 155ms after impact

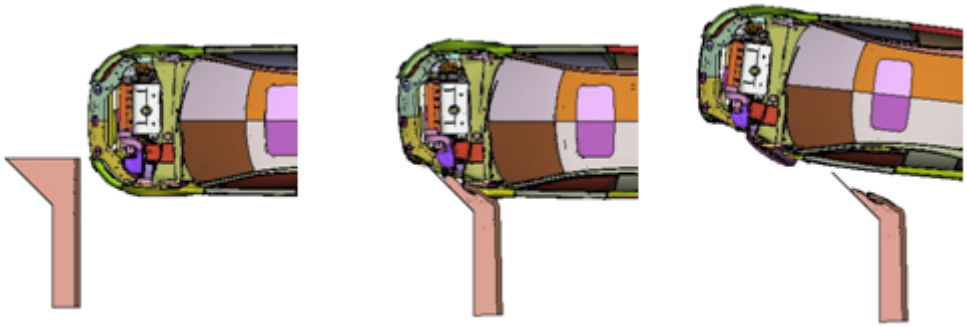

Figure 4.30 Simulation of a 25% overlap crash at 75 km/h with angled support structure. Left: before impact; Middle: 65ms after impact; Right: 155ms after impact

For both cases, the results show that the car is prevented to be caught by the truck wheel but the behaviour of the car during the crash is a lot different to the results shown in Section 4.4.2.

The Figure 4.29 shows that using the straight support structure, the left side of the car is caught by the back plate. This prevents the car to hit the truck wheel but generate to negative effects. The first one is that since the car side is caught by the back plate, it leads to a severe deformation of the car. The second effect is that the car starts to rotate around the vertical axis.

The Figure 4.30 shows a totally different behaviour of the car. While crashing into the honeycomb crash nose and thanks to the bent support structure, the car starts to glance off and keeps moving forward. Also, the car deformation is much lower than with the straight support plate.

Since the total truck increased length has been limited to 900 mm, one needs to notice that with the bended support plate the amount of honeycomb has to be reduced and this affects the energy absorption mainly for bigger overlaps. The following graphs show the comparison between the car intrusions and deformations for these two models with a closing speed of 85 km/h, see Figure 4.31.

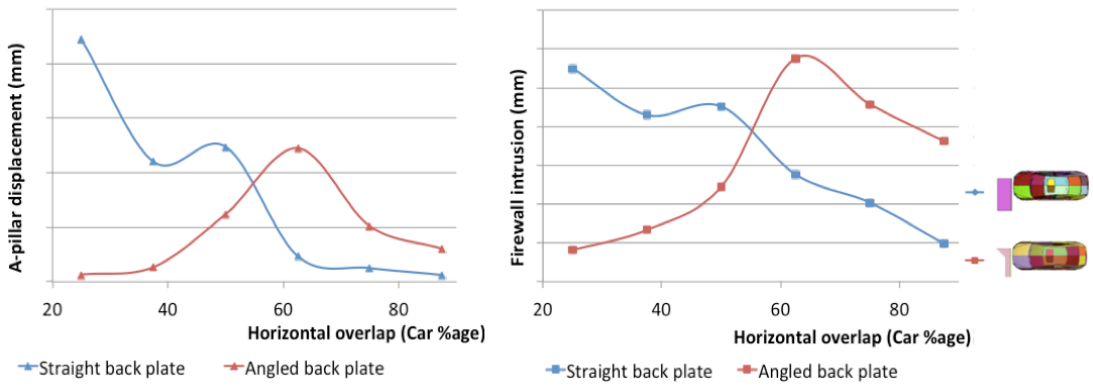

Figure 4.31 A-pillar displacement and firewall intrusion for a closing speed of 85 km/h and different overlaps

From the figure above, it can be seen that the two models give really different results depending on the horizontal overlap. For larger overlaps, the straight support plate model leads to lower car deformations due to the higher amount of honeycomb. Whereas for small overlaps, the angled support plate model has better results since the angle provide the car to glance off. The same trends have been seen concerning the results of the OLC values.

The effects of having an angled support plate for small overlap collisions, with and without honeycomb, can be seen in Figure 4.32. This demonstrates that having this type of angled support promotes the glance off effect.

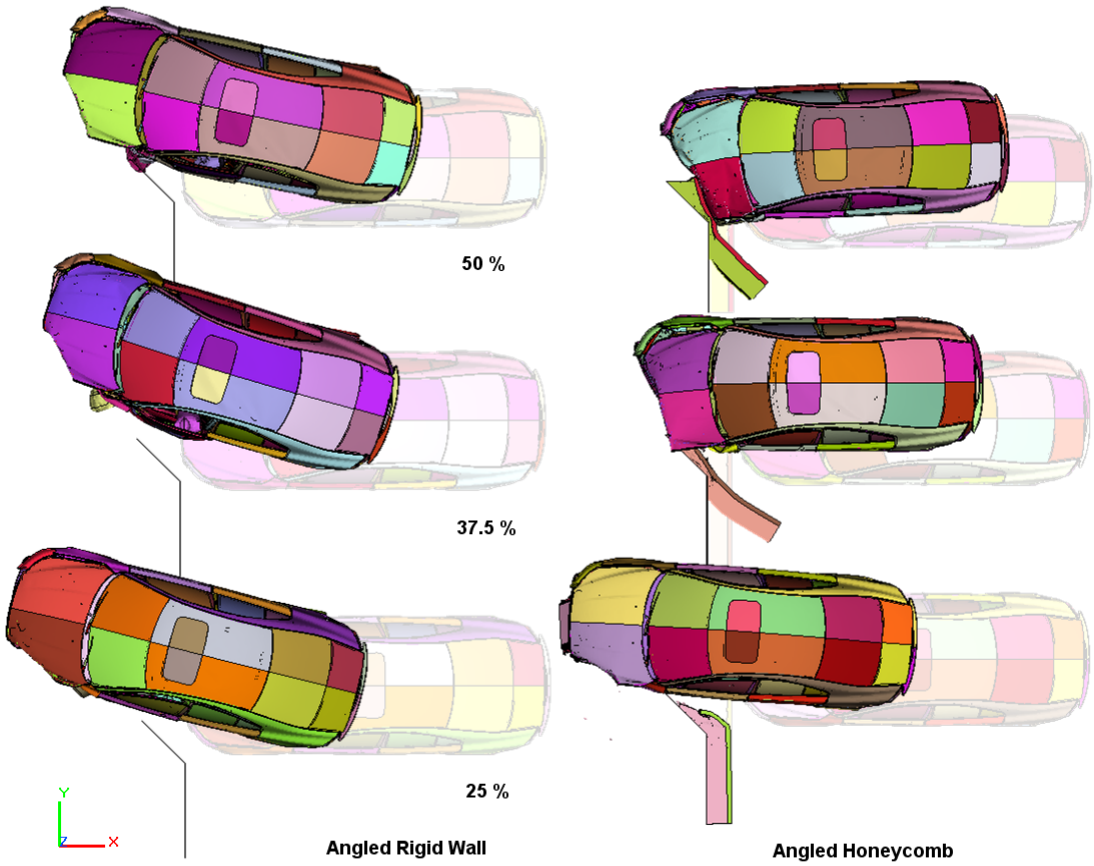

Figure 4.32 Glancing off effect, with and without honeycomb, for different small overlap collision at 75 km/h

4.5.2 External shape

From the simulations using the round external honeycomb shape, the influence of the external shape has been investigated. Simulations #21 and #22, see Appendix 8.2.

The following graph show the comparison between the two model results of the simulations of different overlap crashes with a closing speed of 75 km/h. The different curves show the A-pillar displacement, the firewall intrusion and the OLC values, see Figure 4.33.

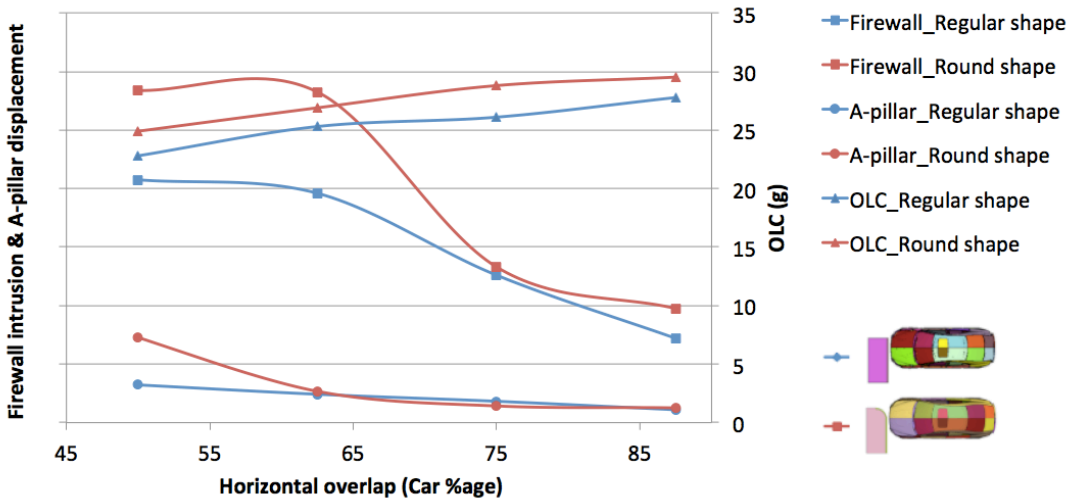

Figure 4.33 Firewall intrusion, A-pillar displacement & OLC values as a function of the horizontal overlap. Closing speed of 75 km/h.

It can be seen that for overlaps higher than 75%, the car deformation results are nearly identical but once the horizontal overlap decreases, the firewall intrusion for the round shape goes up by almost 50% compared to the regular shape. The same can be seen for the A-pillar displacement for a 50% overlap crash. Concerning the OLC for the round shape HC structure, the values are between 5% and 10% higher. As it was expected, the decreased amount of honeycomb material has an effect on the crash nose efficiency.

The Figure 4.34 shows the energy absorption repartition between the car and the HC structure depending on the model (round or normal shape). The simulation load case was a 75% overlap collision with a closing speed of 75 km/h and the two different models compared are the normal shaped and round shaped 900 mm-length HC structure.

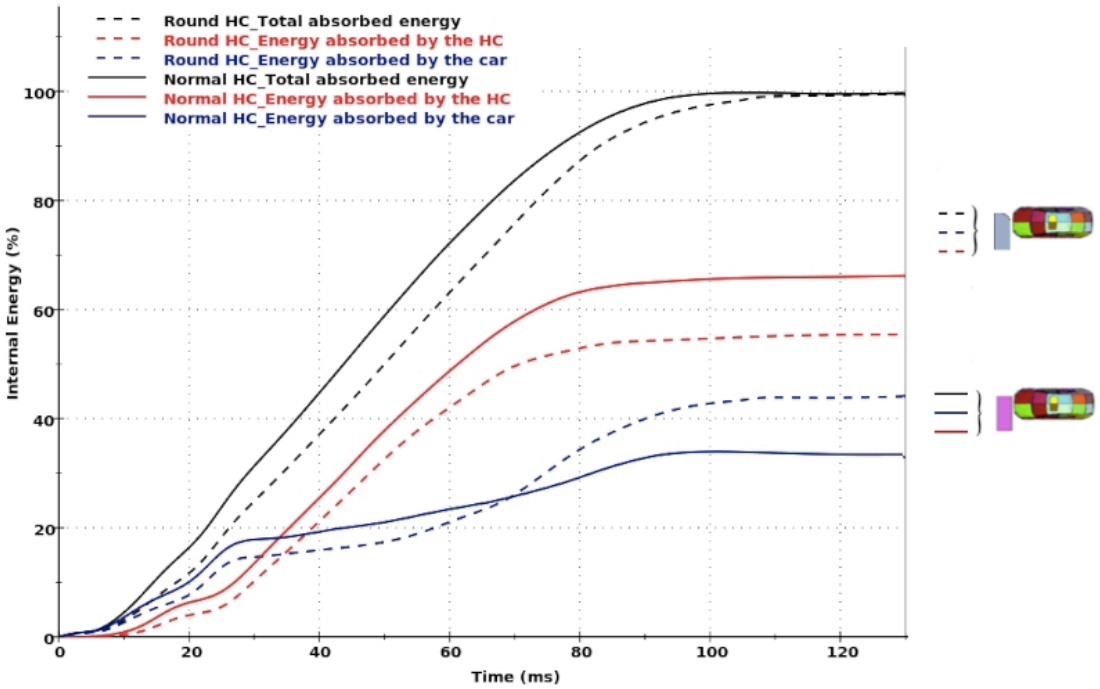

Figure 4.34 Energy absorption repartition for a 75% overlap collision at 75 km/h

Once again, it can be seen that since the amount of honeycomb material is lower for the round shaped HC structure its energy absorption is also lower. For this round shape model, the energy absorption repartition is 45%-55% (car-HC) whereas for the normal shaped HC this repartition is 33%-66%, see Figure 4.34.

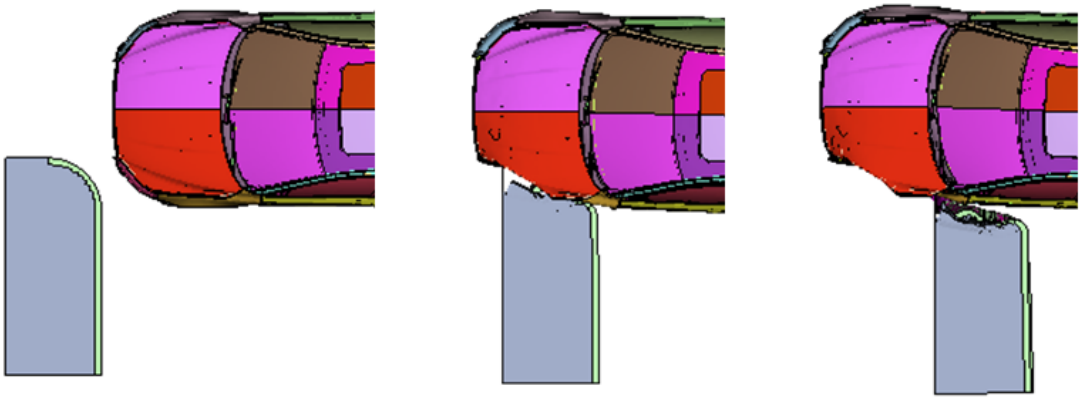

Figure 4.35 Effect of round external shape honeycomb with 25% overlap and at 65 km/h. Left: before impact; Middle: 65ms after impact; Right: 115ms after impact

For this case as for the rectangular honeycomb shape, the car is caught by the back plate and therefore prevented the car to be caught by the truck front wheel. Add to this, the expected deflection of the car was almost none or similar to the rectangular honeycomb structure as shown in Figure 4.29. Simulations #23 and #24, see Appendix 8.2.

The only beneficial benefit from the round external that can be seen from Figure 4.35 is that the behaviour of the car to rotate has been decreased as a result to a slight deflection of the car during the beginning of the honeycomb deformation.

4.6 Forces into the support structure

4.6.1 Force distribution from the HC structure

In order to have a relation in how the honeycomb distributes and therefore reduces the forces that need to be supported, the comparison between the same case scenarios has been made for a 75% overlap and a closing speed of 75 km/h. The same colour scale is used for the Figure 4.36 and Figure 4.37. Simulations #25 and #26, see Appendix 8.2.

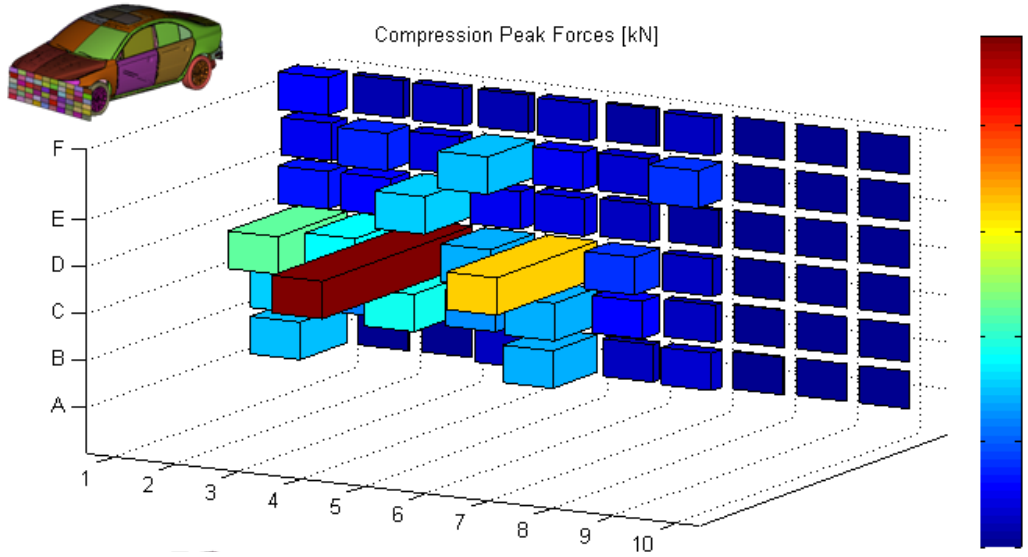

Figure 4.36 Normal peak forces at 75 km/h for a rectangular rigid with 75% overlap

Without honeycomb, three peak values can be seen. These peaks are located where the car engine hits the rigid wall followed by the two peaks on the sides where the car longitudinal crash boxes are located, see Figure 4.36. For different overlaps the peak force location follows the overlap offset.

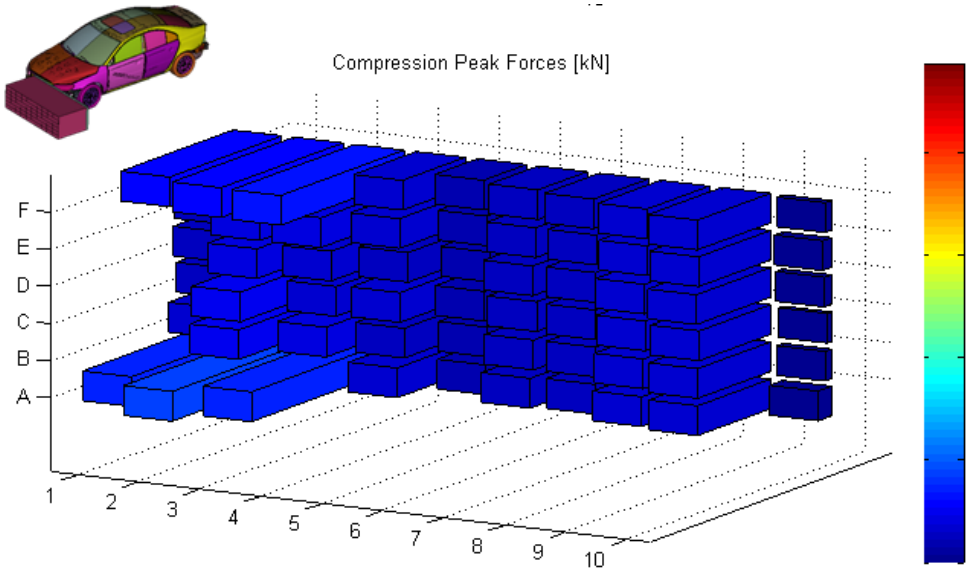

Figure 4.37 Normal peak forces at 75 km/h for a 900 mm-length honeycomb structure

In contrast with the addition of honeycomb material, it can be seen that the forces are distributed along the entire area of the structure. The maximum compression peak value is more than 80% inferior to without honeycomb.

On the other hand, the values in tension increase for the part of the structure that is opposite to the crash, as shown in Figure 4.38. These tension forces are lower than 20kN and are generated by the honeycomb behaviour.

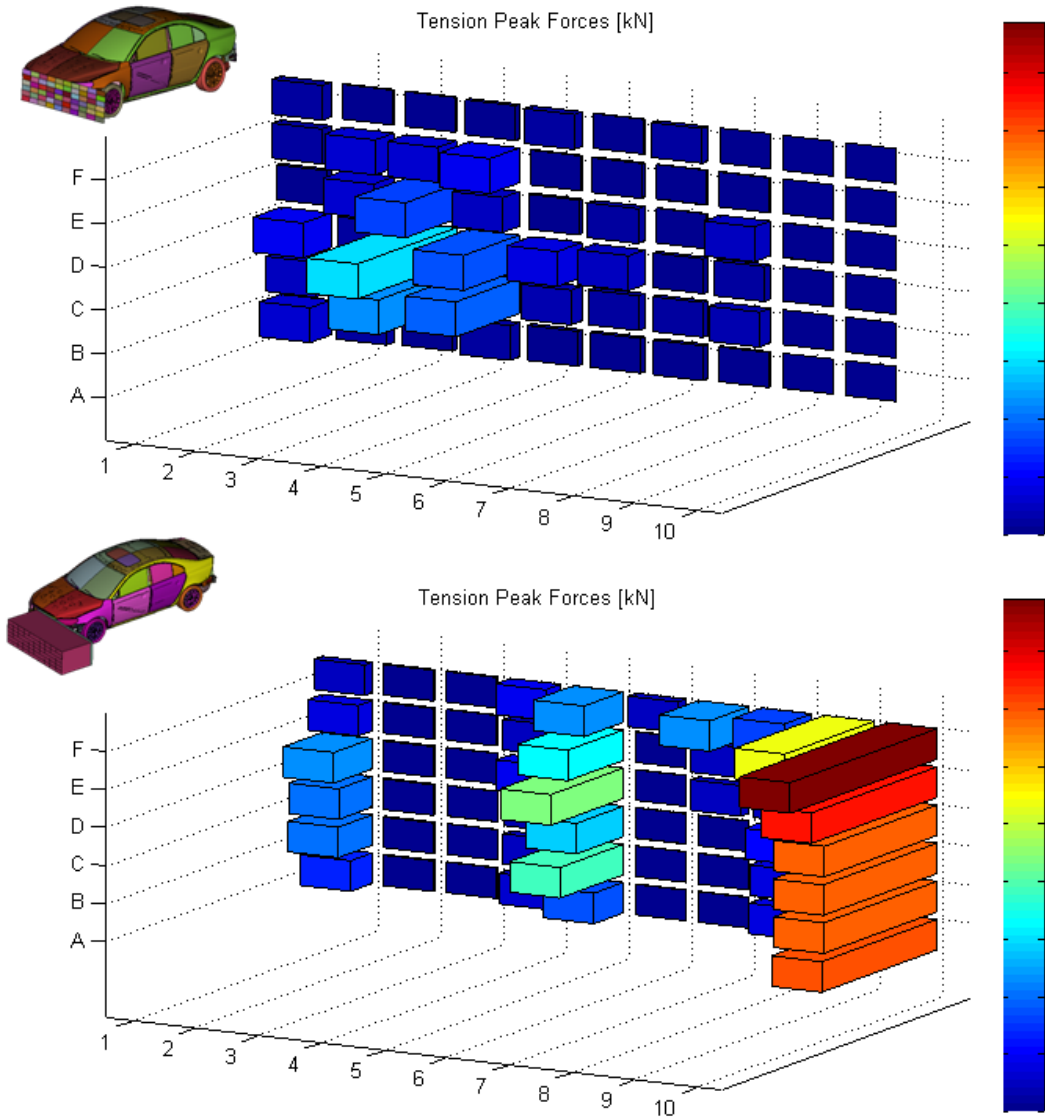

Figure 4.38 Normal peak forces at 75 km/h for a rectangular rigid wall and a rectangular 900 mm honeycomb structure. The same colour scale is used

In order to compare the values due to the force distribution presented for the honeycomb structure, it was necessary to consider that sum of the peak values per cell column. As shown in Figure 4.39, the values after the addition of a 900 mm structure decrease significantly the forces acting in each zone (column). With the honeycomb structure, the maximum peak is around 160kN compared to nearly 450kN without.

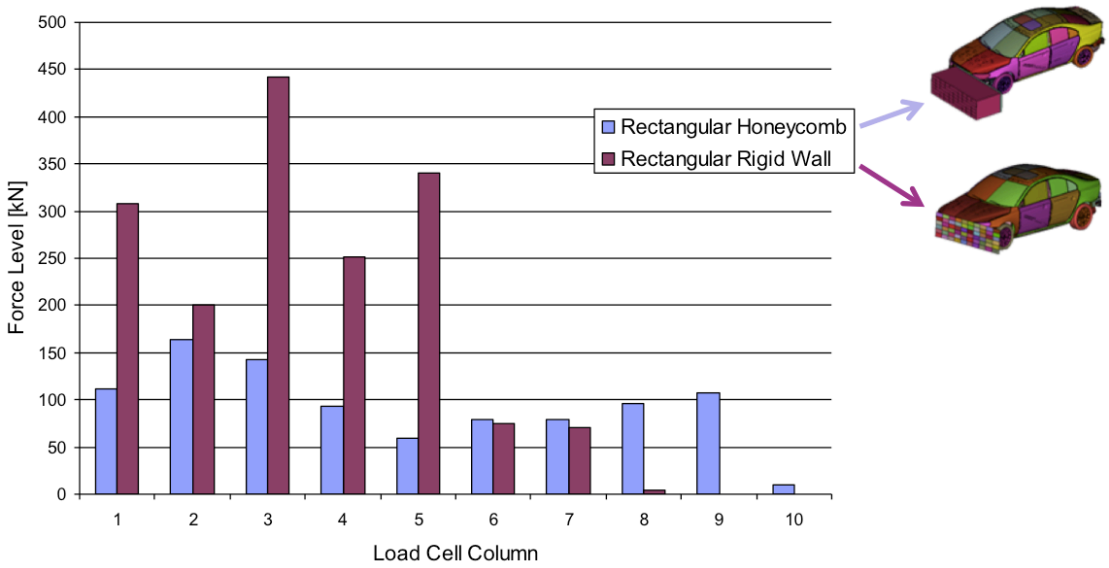

Figure 4.39 Compression peak force values per cell column for 75% overlap and 75 km/h

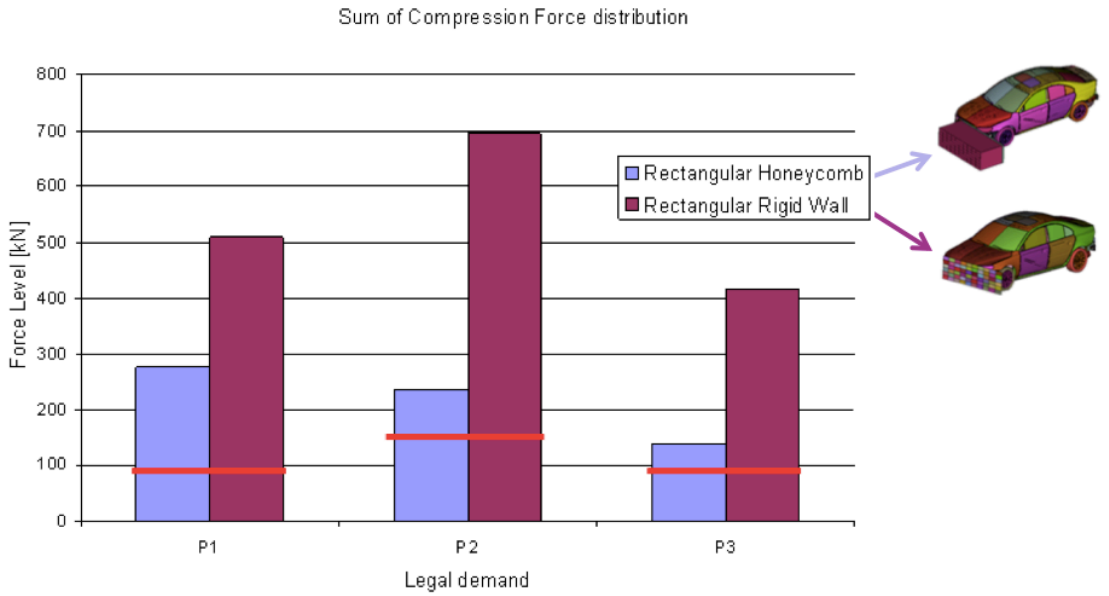

Figure 4.40 Peak tension force values per cell column for 75% overlap and 75 km/h

The legal demands for P1, P2 and P3 are 80, 160 and 80kN respectively, although this forces are not applied at the same time, the values shown in to Figure 4.40 with the addition and without honeycomb material are still higher than the requirements.

4.6.2 Maximum peak forces

The first results show the maximum peak forces that occur during a full frontal head-on collision between the car and the load cell plate without the honeycomb structure in front (rectangular shaped rigid wall), see Figure 4.41. Simulations #27, #28 and #29, see Appendix 8.2.

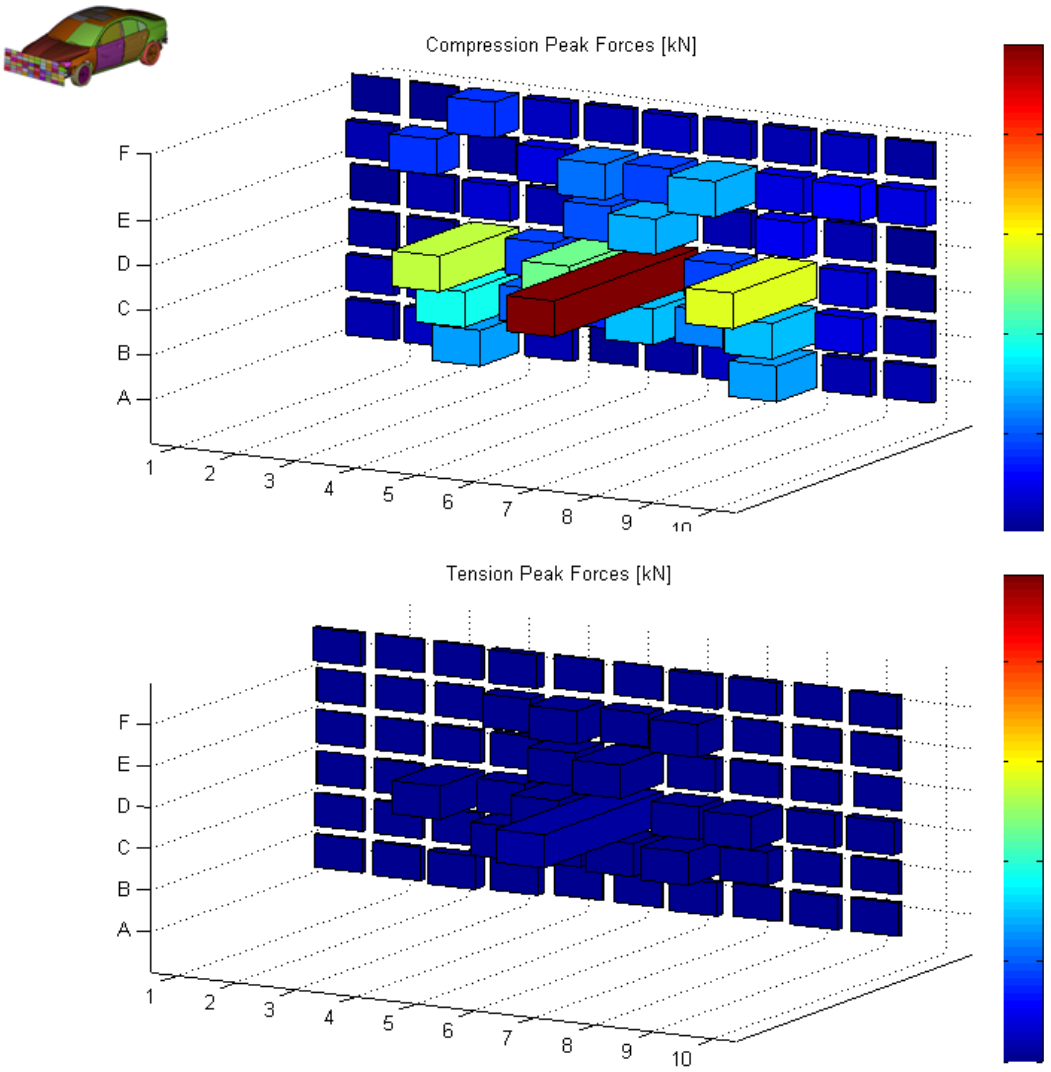

Figure 4.41 Maximum normal peak forces for full frontal crash at 75 km/h. The same colour scale is used.

For this load case, the normal force peaks are located in the region where the car engine hits the load cell and on both sides of it where the car longitudinal crash boxes are located. The tension force peaks are really low compared to the compression ones. For different overlaps the peak force location follows the overlap offset.

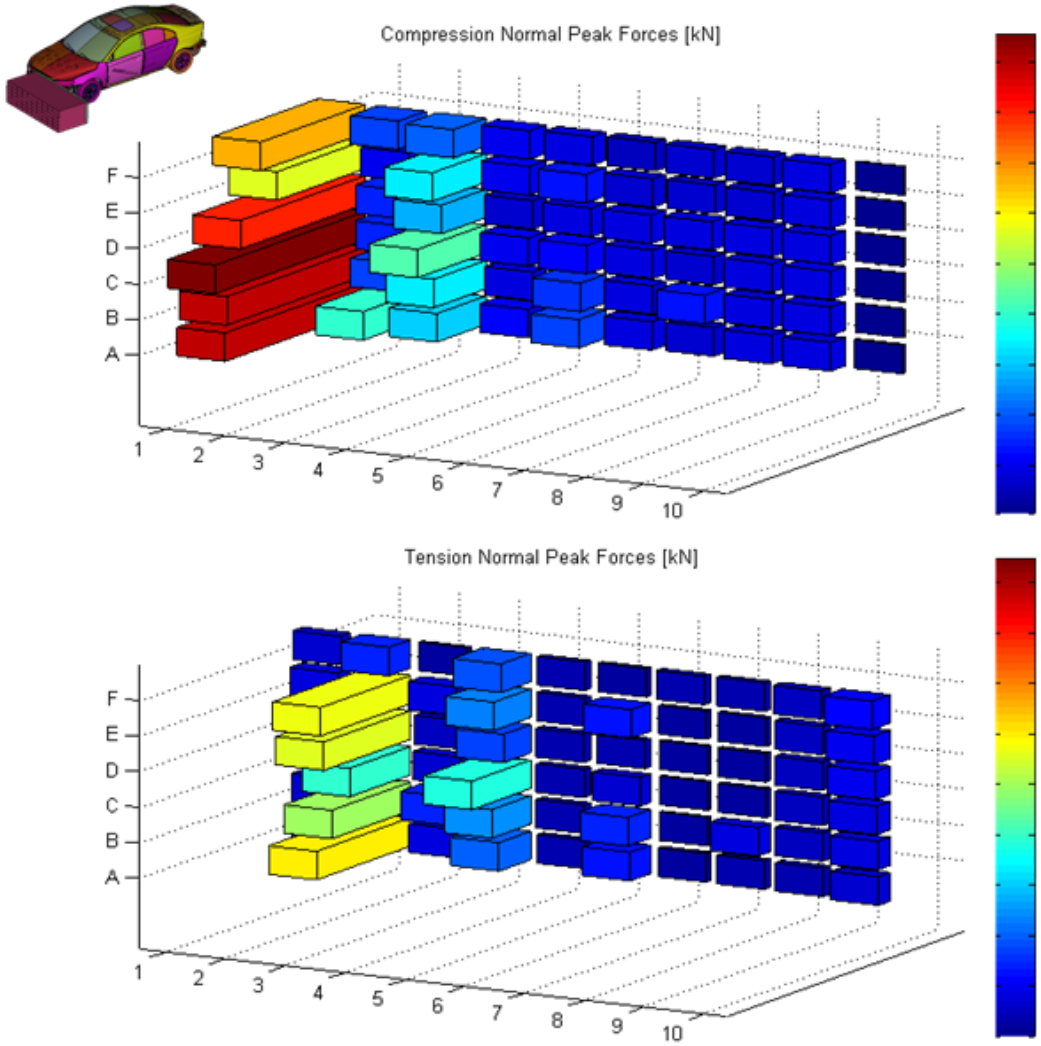

Figure 4.42 Maximum normal peak forces at 75 km/h using the rectangular honeycomb structure. The same colour scale is used. Maximum peak values for 25, 50 and 75% overlap

By adding the rectangular honeycomb structure the force levels are reduced and distributed vertically. For this load case with a 900 mm honeycomb structure is added the maximum force was reduced by 22,2% compared to the rigid wall load case, see Figure 4.42. The results with an increased impact speed (85 km/h) are shown in Appendix 8.3.

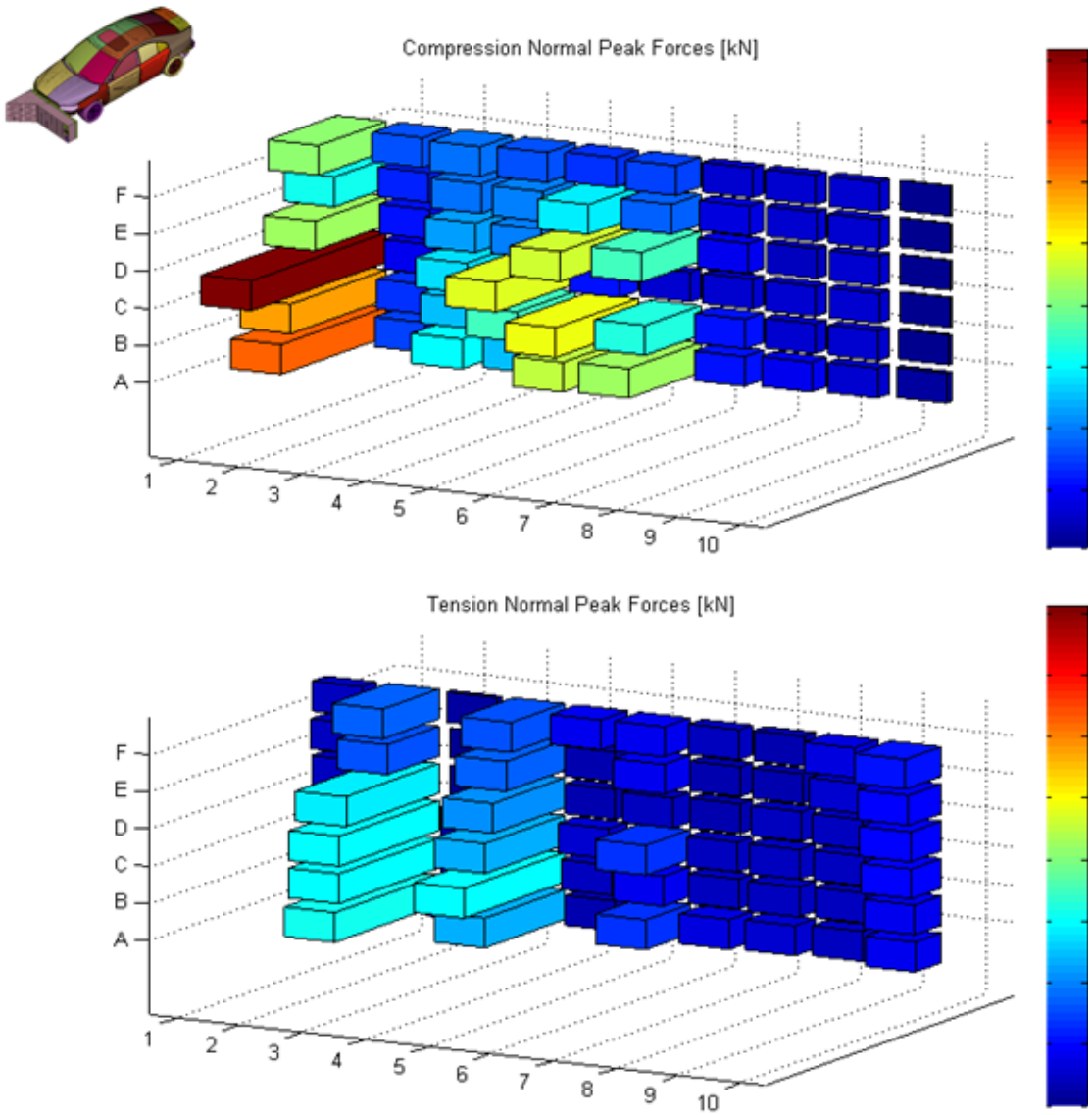

Figure 4.43 Maximum normal peak forces at 75 km/h using the angled honeycomb structure. Maximum values for 25, 50 and 75% overlap. The same colour scale is used

The effect of having an angled back plate support is shown Figure 4.43. The forces are reduced even if the amount of honeycomb material is reduced compared to the rigid wall shown in Figure 4.41. This is related to the fact that the 45° degree angled support structure enhances the glance off effect.

5 Discussions

- **Use of the simplified truck model**

The honeycomb crash nose has first been placed in the front of the truck models but it has been quick decided that a simplified truck model should be used, see Section 3.2.3. Due to the complexity of the model using the full truck models and the crash nose, the calculation time for each simulation was between 20 and 30 hours and it has been considered to be too long to do the truck nose optimisation since many simulations had to be run. This is why the simplified truck model has been used.

The use of this simplified has been validated by comparing the results given from both the simplified and full truck model, see Section 4.1.1. The results concerning the energy absorptions and car deformations are really close and since the OLC values were higher for the simplified model but following the same trend, it was considered that the simplified truck model could be used for the stiffness optimisation of the crash nose.

On the other hand, the models with the honeycomb structure mounted on the full truck model have been used also for few simulations, for example to compare the difference of the results depending on the truck model used (FHT or RHT), see Section 4.4.1.

- **Honeycomb material development**

For the development of the honeycomb material as an energy absorbing structure, the reference model used was the *Moving Deformable Barrier Specification* [18], and since this model is designed for low speed impacts; the models used for this study had to be tuned to have the proper element deformation for higher impact speeds.

For the optimisation of the honeycomb crash structure with the different lengths, it has decided to start the optimisation using a closing speed of 65 km/h, since this was the speed at which the car was starting to have rather high deformations for the reference car-to-truck load cases. Then, higher speeds have been used aiming to find the critical impact speed when the honeycomb structure was added. As it has been said just above, the honeycomb material model used has not been made for high impact speeds and therefore the maximum impact speed for the optimisation was 95 km/h for model stability purposes.

When the honeycomb barrier has been used for smaller horizontal overlap simulations, either mounted on the truck front or using the simplified model, the behaviour of the honeycomb deformation was again giving some stability problem and therefore, the maximum impact speed that was used was 75 km/h. For some load cases, the results were partly wrong and therefore not used in the results.

- **Honeycomb optimum stiffness**

From the optimisation of the honeycomb stiffness results, see Section 4.1.2, it can be seen that the shorter the honeycomb structure, the higher the optimum honeycomb stiffness. Therefore, the advantage of a longer structure is not only that it can absorb more energy but it also reduces the optimum stiffness of the honeycomb. This point is very important when considering lighter car models. Since their front deformable structure are design for a lower weight, their crush strength is lower and therefore the force needed to crush them also. If the honeycomb material crush strength is higher

than the car front one, that means that the car will be deformed before the honeycomb structure and that means that the benefits are reduced.

- **Robustness checking**

The robustness checking of the honeycomb structure has been reduce to one simulation with an angled impact and three simulations using the lighter car model. Since the study has been focussing on the effect of the shape of this structure, it was decided first to go further on this subject and that a later robustness checking using more different load cases would be done once the optimum shape on this honeycomb structure will be found. Nevertheless, it was shown with the few different load cases done in that study that the honeycomb structure has also benefits for angle impacts and lighter cars, see Section 4.2.

- **Critical impact speeds**

It is really interesting to notice that the values of the impact speeds calculated using the honeycomb nose simulation results and the ones from the analytical methods are close to each other. For instance, without honeycomb the critical speed is around 77 km/h from the simulation and about 80 km/h from the calculations. The same can be seen for the critical speeds for the three different crash structure lengths, see Section 4.3.

The main difference between the two models was that for the honeycomb nose, the crush force is proportional to the surface engaged in the deformation whereas for the analytical model, this crush force of the FUPS is constant.

When the maximum energy that the honeycomb can absorb has been estimated from the simulations, it was decided to take this value for the honeycomb nose optimised for an impact speed of 95 km/h even if for higher speeds the energy absorbed could be higher with an increased stiffness but then the crush strength would be too high and in case of a crash with a lighter car, the crush force would higher than the car front deformable zone and therefore the advantages of this honeycomb structure would de cancelled if it is not deformed before the car.

It can be noticed also that the critical speed increase from a 300 mm-length to 900 mm-length honeycomb structure is only 12 km/h even if the length is increased by 600mm.

- **Round shaped honeycomb structure model**

As it has been said in Section 3.2.2, the radius used for the round shaped honeycomb structure model was 500mm. This value has been chosen based on aerodynamic hypothesis since it is said to be an optimum value.

Even if the round external shape reduces the amount of honeycomb and therefore the energy absorption, it can be thought that for future aerodynamic demands the eternal shape will not be square. Add to this, for vulnerable road users (cyclists and pedestrians), a rounded shape could be useful to deflect them instead of run over. Also the front shape is more likely not to be square to gain in term of manoeuvrability. All these parameters have not been taken into account for this study but could be in a further study.

- **Angled support nose model**

For the design of the angled back plate of the honeycomb nose, it was considered to use a 45° angle and to have this bent situated around 600 mm from the honeycomb structure side, see Section 3.2.2. However, these dimensions were set as start up values to evaluate the effects of this type of support structure.

By comparing the results between the normal 900 mm-length honeycomb and the angled support plate one, it can be seen that both have positives and negative points, see Section 4.5.1. When considering large overlaps (above 50%), the normal shape in more efficient since the amount of honeycomb is much larger, therefore the car deformations are lower and the same for the OLC. But considering small overlaps, this is the opposite. Since the angle back plate structure provides a glancing-off effect on the car, the car deformation are in these cases much lower and the same for the OLC. It could be interesting to calculate the OLC with the longitudinal and lateral acceleration since the deflection lateral acceleration is perhaps not neglectible.

This is why it seems from the first results that a kind of mix between those two models could be a good solution. Therefore an optimisation of the dimensions of the bent plate would be interesting in order to evaluate the influence of these parameters on the effectiveness of the honeycomb structure. The aim would be to provide a glance-off effect for small overlaps in compromise with a good energy absorption for big overlaps.

- **Additional load cell back plate**

The addition of a load cell plate was determined by the fact that it was interesting to measure the forces that have to be supported behind the new front structure. Since, it has been seen that the addition of the honeycomb crash nose efficiency is linked to the fact that there is a good support behind it, see Section 4.4.1. Therefore, it d suppose that this new structure will be mounted on a new truck front structure different that the one existing today and from the perspective of this new design, it is compulsory to know the efforts that this new design truck front structure should be able to support. For this study, 60 load cells have been used, giving a good overview of what are the forces occurring during the crash. A larger number of cells could provide a more accurate force distribution diagram; nevertheless the values obtained by the current load cell plate provide relevant data.

- **Car-to-truck simulations with small horizontal overlaps**

During this study, some problems have been encountered for the simulations of crashes with small horizontal overlaps (lower than 37,5%). The maximum impact speed that has been used was 65 km/h because the simulations were not ended when using higher impact speeds. This is why not so many results were available for these load cases. One hypothesis about this is that the model of the wheel suspensions and tires of both the truck and the car models should be more accurate since they are the main parts engage during small overlap crashes and it was seen that their behaviour was causing problems during the simulation.

6 Conclusions

The usage of the honeycomb material gives the alternative to create a light-weight truck crash nose with energy absorbing characteristics. As it has been said, one of the main factors limiting the efficiency of the FUPS is their length. The longer they can be, the more energy they can absorb.

For the three different lengths evaluated, the addition of a 300, 600 and 900 mm frontal HC structure represents a reliable solution in order to reduce the A-pillar and firewall deformations for the passenger car. Even though the OLC increases for overlaps below 62,5% the values will not represent a significant drawback of the new frontal structure since they are still below the average, see Figure 3.14.

For the current truck, the critical speed has been estimated to be around 72 km/h for the flexible truck and 77 km/h for the rigid truck. By the addition of the HC the critical impact speed would be raised

- To 95 km/h with a 300 mm-length HC structure (+27%)
- To 102 km/h with a 600 mm-length HC structure (+36%)
- To 107 km/h with a 900 mm-length HC structure (+43%)

By raising the critical impact speed from 75 km/h to 107 km/h could reduce the car occupant fatalities due to head-on HGV collisions by 10%. If all trucks were equipped with a new front structure, an estimate is 350 car occupant lives saved per year in Europe, see Appendix 8.4.

For a 900 mm-length honeycomb structure, it has been found that the optimum honeycomb material stiffness would be between 0,288MPa and 0,365MPa depending of the closing speed used for the optimisation. Using such stiffness, the initial crush forces of the honeycomb are between 300 and 350kN and then increasing since the crush force is proportional to the amount of honeycomb being deformed. This crush force is very important because the crash nose should be compatible with lighter car too. If the crush force of the honeycomb crash nose is higher than the force created by the front car deformation then the car will be deform before the honeycomb reducing its efficiency. This is why the robustness checking is important.

In order to have a good efficiency of the crash nose structure, three key factors have to be fulfilled: a good geometrical compatibility, a good load distribution and a good support behind the truck crash nose.

- The geometrical compatibility is important to get a good deformation of the car front structure. As it as been done in this study, this can be achieved with a low ground clearance of the truck (around 200mm) to catch the lower car bumper. It seems also that a height of this truck crash structure should be around 600 mm to catch the whole car front structure, see Figure 3.16.

- The load distribution on the honeycomb allows deforming a larger amount of honeycomb material instead of having a local deformation. In this study, this load distribution has been achieved using steel plates in front and at the rear of the honeycomb structure. Even if these steel plates represent around 60% of the 900 mm-length structure, their use is really important.

- The back support of for the honeycomb structure plays an important role in the energy absorption capabilities of the honeycomb and the car deformation. As described in section 4.4, a rigid support structure leads to a more uniform deformation of the honeycomb and therefore the amount of energy absorbed by the honeycomb is higher. For small overlaps, it is required to consider that the back support structure is a critical factor as mentioned in section 4.4.2. If the back support strength is not able to handle the forces at the moment of impact, this can result in the case where the passenger engage with the truck frontal wheel leading to severe car intrusions.

In order to improve the small overlap crashes and avoid the situations where the car hits the front wheel of the truck or it gets engaged by the support structure for small overlaps as described in section 4.5.1, it has been shown that an angled back support structure promotes a glancing off effect of the car. This deflection of the car for small overlaps seems to be a key factor for reducing the severity of the crash. Since the car is glancing off, the collision could be avoided. It is important to notice that using an angled back plate reduce the extra length available and therefore the amount of honeycomb. This has for consequences higher car deformations and OLC compared to the normal 900 mm-length crash nose for larger overlaps. Therefore, this back support plate shape needs to be design with a good compromise between this angle plate beneficial for small overlap and the normal shape better for large overlaps.

On the other hand, the external shape of the honeycomb evaluated in Section 4.5.2, resulted not to be a determination factor. For large overlap, the difference with the normal honeycomb external shape was nearly none. In case of small overlap crashes, the car deformations were higher since the amount of honeycomb is reduced due to the round shape, the amount of energy absorbed is lower. Therefore, if it is not for aerodynamic or other purposes, the external shape should be maximizing the amount of honeycomb (rectangular for instance).

7 Future work

7.1.1 Further research about the truck nose design

This study has shown the benefits that an extended truck crash nose could have for reducing the crash severity. As it has been discussed, using the bent back plate provide a glance off effect for small overlap crashes but has lower benefits for larger overlaps. Therefore, a deeper optimisation should be done concerning the back plate shape in order to find a good compromise for every overlaps. This deeper study should be investigating the effects of different angles for the back plate and also the length of this bent part. This next optimisation should also take into account small overlap crashes with an angle impact.

Once an optimum shape will be found, a deep robustness checking will be needed to access the efficiency of the new truck structure for different crash configurations: vertical offset, impact angle, lighter car. Off course the next step would be to be able to compare the simulation testing with real test.

Another point that could be investigated would be to give an initial speed to the truck since for this study had always no initial speed. This would provide results about the behaviour of the car after crashing into the truck.

7.1.2 Improve the accuracy of the simulations

During this study, some limits have been encountered for different simulations, concerning either the car and truck FE models or the honeycomb material model. Therefore, it seems that for small overlap crashes at high speeds, it would be necessary to used more detailed models for both the truck and car especially the wheels and wheel suspensions since there were some problems for the small overlaps simulations.

Concerning the honeycomb material, it has been modelled using solids elements that had the material properties as the honeycomb material and once again some problems have been seen with high-speed crash simulations. Therefore, a new model of the honeycomb structure could be developed. This new model could be done using a discrete beam method since it is said to “ensure high stability even under severe deformation of the honeycomb structure without any problems of numerical instability” [22]. This king of model would perhaps be more realistic and more stable for the different simulations.

7.1.3 Other benefits possible from this crash nose

In this study, the effects of this new frontal structure have been limited to the crash severity for the car but a lot more could be done.

To begin with, studies have shown that this structure could be used for improving the protection of vulnerable road users such as cyclist or pedestrian.

Then, this new frontal structure could also be used for improving the aerodynamic of the truck by optimising the nose shape to decrease the drag coefficient and improve the airflow around the truck.

Last, an extended front of the truck could improve the truck occupant protection as well in collisions between the truck and heavier objects as other trucks for example.

8 Appendix

8.1 Honeycomb material description

Bumper Element Honeycomb Material

The bumper element honeycomb is manufactured out of aluminum 3003, with a cell size of 6,35 mm, a density of 83,0 kg/m^3 ± 4 kg/m^3, and a crush strength of 1690 kPa ± 103 kPa, measured in accordance with the certification procedure described in US Department of Transportation, NHTSA, Lab Test Procedure for FMVSS No. 214 "Dynamic" Side Impact Protection, TP214D Appendix C TP214D-07 C-1.

Main Honeycomb Block Material

The main honeycomb block is manufactured out of aluminum 5052, with a cell size of 9,5 mm, a density of 25,6 kg/m^3 ± 4 kg/m^3, and a crush strength of 310 kPa ± 17 kPa, measured in accordance with the certification procedure described in US Department of Transportation, NHTSA, Lab Test Procedure for FMVSS No. 214 "Dynamic" Side Impact Protection, TP214D Appendix C TP214D-07 C-1.

In order to optimise the aluminum honeycomb material used, it was chosen to scale the yield strength function in the x, y and z directions. In Figure 8.1 are shown the material strength function for their respective direction.

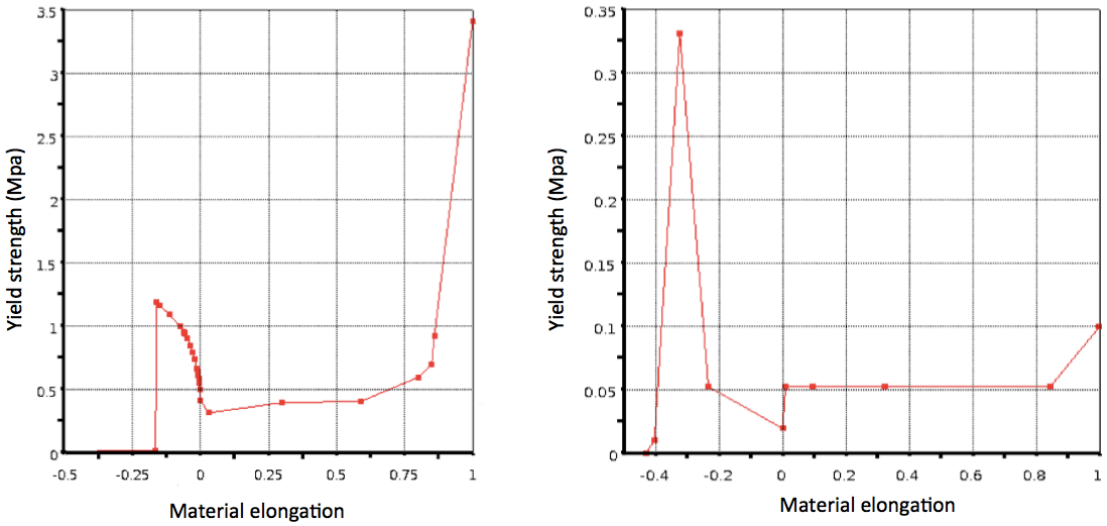

Figure 8.1 *Yield strength characteristics of the main honeycomb material. Left: σxx ; Right: σyy and σzz*

8.2 Sum up of the FE simulation load cases used

		Car model	crashing to	Truck model			Honeycomb nose			Simulation configuration	
Report section	Simulation	S80/lighter car	Truck/Simplified model	Flexible /Rigid	Rear fixed /Not fixed	Weight (12 tonnes or fixed)	Yes / No	Length	Special shape/ Comment	Initial car velocity	Horizontal overlap
4.1.1	#1	S80	Truck	Rigid	Not fixed	12 tonnes	Yes	900 mm		65 to 95 km/h	75%
	#2	S80	Simplified model		Not fixed	12 tonnes	Yes	900 mm		65 to 95 km/h	75%
4.1.2	#3	S80	Simplified model		Not fixed	12 tonnes	Yes	300, 600 and 900mm		65 to 95 km/h	75%
4.1.3	#4	S80	Truck	Flexible	Fixed		No			65 km/h	37,5 to 87,5%
	#5	S80	Simplified model		Fixed		Yes	900 mm		65 km/h	37,5 to 87,5%
4.2.1	#6	S80	Truck	Flexible	Fixed		No		12,5° impact	75 km/h	75%
	#7	S80	Simplified model		Fixed		Yes	900 mm	12,5° impact	75 km/h	75%
4.2.2	#8	Lighter car	Truck	Flexible	Fixed		No			56 to 75 km/h	75%
	#9	Lighter car	Simplified model		Fixed		Yes	900 mm		56 to 75 km/h	75%
4.4.1	#10	S80	Truck	Flexible	Not fixed	12 tonnes	No			65 km/h	65%
	#11	S80	Truck	Flexible	Fixed		No			65 km/h	65%
	#12	S80	Truck	Rigid	Not fixed	12 tonnes	No			65 km/h	65%
	#13	S80	Truck	Rigid	Fixed		No			65 km/h	65%
	#14	S80	Truck	Flexible	Not fixed	12 tonnes	Yes	900 mm		65 to 85 km/h	75%
	#15	S80	Truck	Rigid	Not fixed	12 tonnes	Yes	900 mm		65 to 85 km/h	75%
4.4.2	#16	S80	Truck	Flexible	Fixed		No			65 km/h	25 & 37,5%
	#17	S80	Truck	Flexible	Fixed		Yes	900 mm		75 km/h	25 & 37,5%
	#18	S80	Truck	Rigid	Fixed		Yes	900 mm		75 km/h	25 & 37,5%
4.5.1	#19	S80	Simplified model		Fixed		Yes	900 mm		75 & 85 km/h	25 to 87,5%
	#20	S80	Simplified model		Fixed		Yes	900 mm (angled support)		75 & 85 km/h	25 to 87,5%
4.5.2	#21	S80	Simplified model		Fixed		Yes	900 mm		75 km/h	50 to 87,5%
	#22	S80	Simplified model		Fixed		Yes	900 mm	Round corner	75 km/h	50 to 87,5%
	#23	S80	Simplified model		Fixed		Yes	900 mm		65 km/h	25%
	#24	S80	Simplified model		Fixed		Yes	900 mm	Round corner	65 km/h	25%
4.6.1	#25	S80	Simplified model		Fixed		No			75 km/h	75%
	#26	S80	Simplified model		Fixed		Yes	900 mm		75 km/h	75%
4.6.2	#27	S80	Simplified model		Fixed		No		Full frontal	75 km/h	100%
	#28	S80	Simplified model		Fixed		Yes	900 mm		75 km/h	25, 50 & 75%
	#29	S80	Simplified model		Fixed		Yes	900 mm (angled support)		75 km/h	25, 50 & 75%

Table 8.2 Sum up of the simulation load cases used

8.3 Forces on the back plate for an increased speed

The effect of an increased speed of 85 km/h for the 900 mm-length rectangular honeycomb structure is approximately 21%, see Figure 8.3.

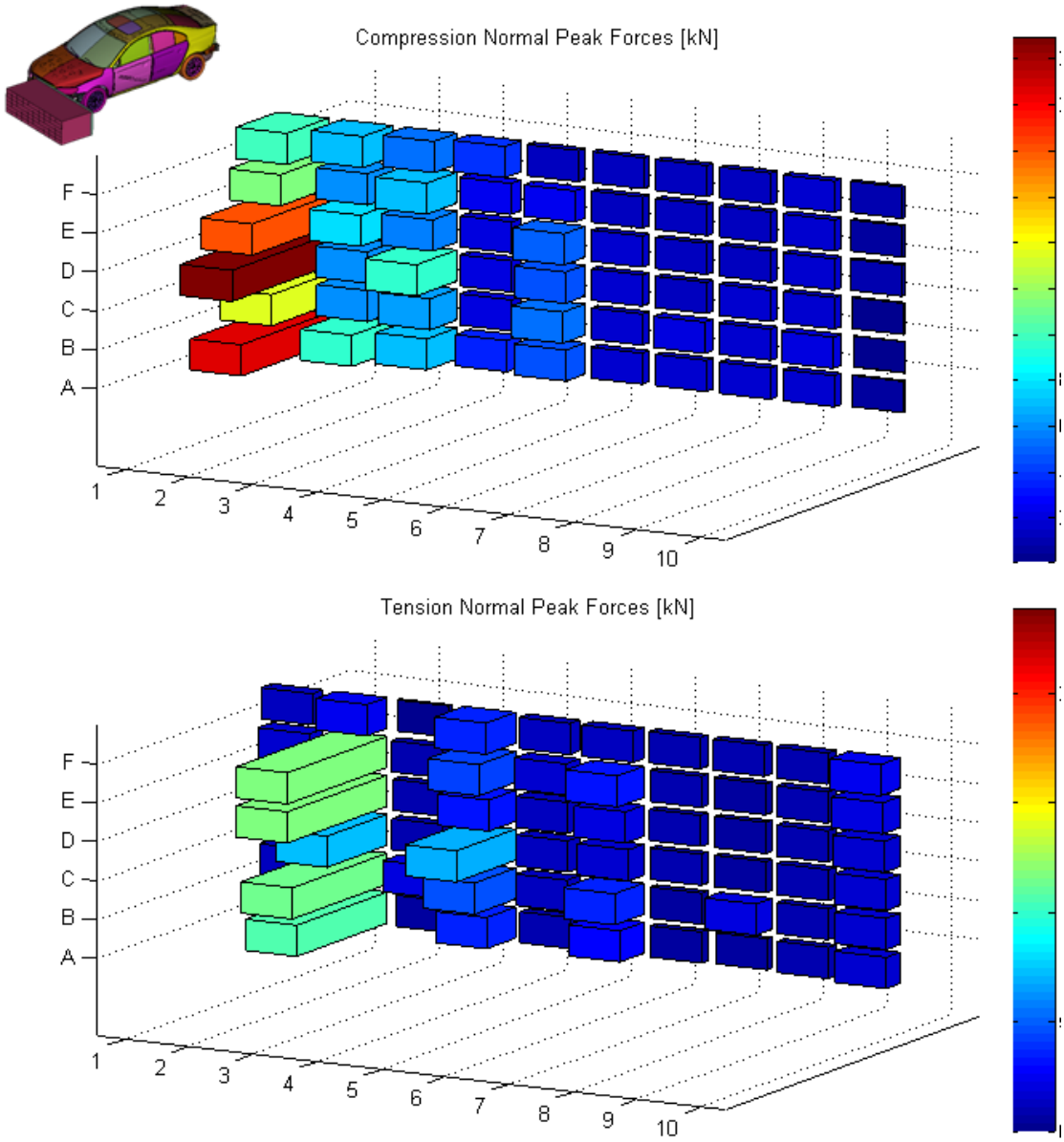

Figure 8.3 Maximum normal peak forces at 85 km/h using the rectangular honeycomb structure. Maximum peak values for 25, 50 and 75% overlap

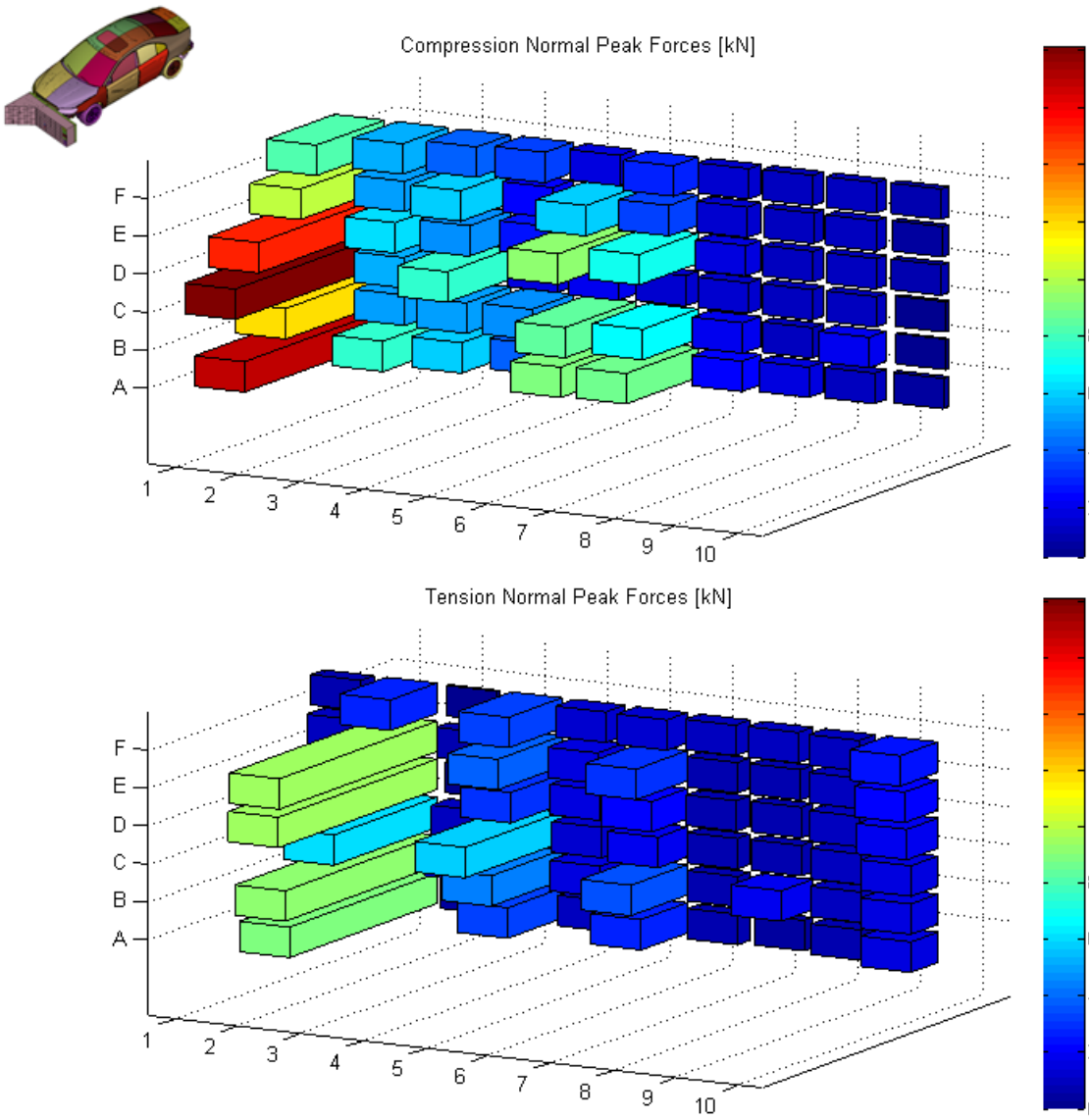

Figure 8.4 Maximum normal peak forces at 85 km/h using the angled honeycomb structure. Maximum peak values for 25, 50 and 75% overlap

With the angled back plate support honeycomb structure, the same results can be seen, that is to say peak force values at the extremities of the load cell plate appearing for the small overlap load case. Else the compression values are less than 50% of the peak appearing for the rigid wall load case at 75 km/h, see Figure 4.41.

8.4 Estimation of the fatality reduction potential

It has been estimated that using a 900 mm-length honeycomb structure could increased the critical impact speed from 75 km/h to 107 km/h. From the cumulative frequency of car occupant fatalities involved in head-on HGV collisions, the fatality reduction potential can be estimated.

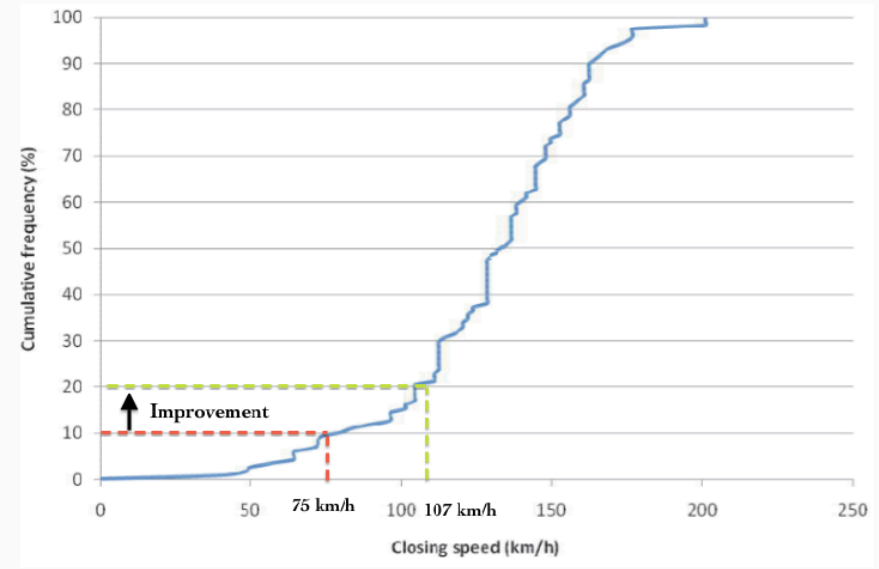

Figure 8.5 Cumulative percentage plot for car occupant fatalities involved in head-on HGV collisions (HVCIS 1997-2006, N=118), taken from [21].

It can be seen Figure 8.5 that around 10% of the fatalities occur at a closing speed below 75 km/h and around 20% at a closing speed below 107 km/h. Therefore, if all trucks were equipped with an effective FUPS, the fatalities could be reduced by 10%. And if the critical speed would be raised to 107 km/h with the new truck front structure, it can be estimated that 10 more percent fatalities could be avoided.

In 2008, around 2600 car occupants have been killed from a collision with a HGV in Europe [1]. A research by Wrige, A. (2003) [3] has shown that 65% of these collisions were involving both the truck front that is to say around 1690 fatalities. Assuming that all trucks would be equipped by a new frontal structure, an estimated 20% of these fatalities could be avoided, representing almost 350 lives per year in Europe. This estimation is not taking into account the truck driver fatalities.

9 References

[1] European Road Safety Observatory (2010): *Traffic safety basic facts 2010.* CARE, EU roads accidents database.

[2] Lundqvist, A. (2005): *Road safety solutions in Sweden.* Swedish Road Administration, Freight transport and intermodality for western African countries Seminar, Ouagadougou, Burkina Fasso, June 2005.

[3] Wrige, A. (2003): *Nobody builds safer trucks.* SIAM conference, New Delhi, India, November 2003.

[4] *IIHS Fatality Facts 2009 Large Truck* (2009), Insurance Institute for Highway Safety [ONLINE].
Available at www.iihs.org/research/fatality.aspx?topicName=Largetrucks&year=2009 [Accessed 6th May 2012].

[5] Robinson, B.J.; Knight, I.; Robinson, T.; Barlow, T.; McCrae, I. (2010): *Safer aerodynamic frontal structures for trucks: final report.* Transport Research Laboratory published project report PPR533, Crowthorne, UK.

[6] Department for Transport (2011): *Consultation on the possibility of allowing an increase in the length of articulated lorries*. Department for Transport, London, UK, 2011.

[7] *Estimating the forces acting during a collision (2001)* The Impact Project; State University of Campinas, Brazil [ONLINE].
Available at: www.fem.unicamp.br/~impact/forca.html [Accessed 6th May 2012].

[8] *Volvo Car Corporation, (2011), 2012 Volvo S60 Body Structure* [ONLINE]. Available at: http://boronextrication.com/2011/08/2012-volvo-s60-body-structure/ [Accessed 24th April 2012].

[9] Wågström, L (2004): *Structural adaptivity in frontal collisions: Impact energy management adapted to crash severity.* Chalmers University of Technology, Göteborg, Sweden.

[10] Malczyk, A. (2007): The influence of recent legislation for heavy vehicles on the risk of underrun collisions. *Verein Deutcher Ingenieure, VDI Berichter*, n 2013, October 2007, pp.299-314.

[11] AB Volvo, (2011), *FUPS - Frontal Underrun Protection System* [ONLINE].
Available at: http://www.volvobuses.com/bus/global/en-gb/volvogroup/safety/fups/pages/fups.aspx [Accessed 24th April 2012].

[12] Lambert, J.; Rechnitzer, G. (2002): *Review of truck safety: stage 1: frontal, side and rear underrun protection.* Monash University Accident Research Centre, Report No. 194, ISBN-0732614937, Victoria, Australia.

[13] Forsman, L. (2002): *Compatibility in truck to car frontal impacts.* 7th International Symposium on Heavy Vehicle Weights & Dimensions Delft, The Netherlands, Europe, June 2002.

[14] Edwards, M. J. et al (2007): *Improvement of Vehicle Crash Compatibility through the Development of Crash Test Procedures*. VC-COMPAT Final Technical Report, Transport Research Laboratory, Crowthorne, UK.

[15] Aleksandra K.; Robert T. (2010): Energy-absorbing FUPDs and their interactions with fronts of passenger cars. *International Journal of Crashworthiness*, Vol. 15, No. 6, pp.635-647.

[16] APROSYS SP2, D2.1.7, (2008): *Guidelines for integrated design and evaluation of advanced vulnerable road user protection systems.* Deliverable report for the EC funded project, APROSYS, 2008.

[17] Huibers, J.; de Beer, E. (2001): *Current front stiffness of European vehicles with regard to compatibility.* Automotive Crash Safety Centre, Netherlands. Paper No. ID#239.

[18] Insurance Institute for Highway Safety (2007): *Moving Deformable Barrier Specification.* N. Glebe Road, Arlington, VA, USA. pp. 2

[19] European New Car Assessment Programme (2011): *Frontal Impact Testing Protocol Version 5.2.* Euro NCAP. pp. 40.

[20] Kübler, L.; Gargallo, S.; Elsäßer, K. (2009): *Frontal Crash Pulse Assessment with Application to Occupant Safety*. ATZ Worldwide, Vol. 111, June 2009, pp.12-17.

[21] Robinson, T.; Chislett, W. (2010): *Commercial vehicle safety priorities – ranking of future priorities in the UK based on detailed analysis of data from 2006-2008.* Transport Research Laboratory published project report PPR486, Crowthorne, UK.

[22] Jost, T.; Heubrandtner, T.; Ruff, C.; Fellner, B. (2008): *A new method to model aluminium honeycomb based crash barriers in lateral and frontal crash load cases.* LS-DYNA Anwenderforum, Bamberg, Germany.

Other lectures

Asadi, M.; Prof. Shirvani, H.; Prof. Sanaei, E.; Dr. Ashmead, M. (2006): *A simplified model to simulate crash behavior of honeycomb.* International conference on advanced design and manufacture, 8th-10th January 2006, Harbin, China.

Castellanos, M.; El-Gindy, M.; Fedishen, C.; Maciejewski, D. and Atahan, A.O. (2010): Truck front underride development: literature survey. *Int J. Heavy Vehicle Systems*, Vol. 17, No. 1, 2010, pp.18-34.

Forsberg, J.; Nilsson, L. (2008): The optimisation process of an energy absorbing frontal underrun protection device. *Int. J. Vehicle Design*, Vol. 46, No. 3, 2008 271.

Hartman, K.; Pritchard, B.; Jennings, K.; Johnson, J.; Knipling, R.; MacGowan, J.; Oliphant, L.; Onder, M.; Sanft, C. (2000): *Commercial vehicle safety – Technology and practice in Europe.* Federal Highway Administration, Report No. FHWA-PL-2000-010, Washington DC, USA.

Johansson, H. (2004): *The truck in the European road safety strategy.* Scania Vice President, International press workshop, Hannover, Germany, September 2004.